# IT'IS FOUNDATION

*Foundation for Research on Information Technologies in Society*

Prof. Dr. Niels Kuster

Director Foundation IT'IS
Professor of Swiss Federal Institute of Technology – ETHZ
Phone +41 1 245 9690 · kuster@itis.ethz.ch

# Development of Procedures for the EMF Exposure Evaluation of Wireless Devices in Home and Office Environments Supplement 1: Close-to-Body and Base Station Wireless Data Communication Devices

*Submitted by:*
Sven Kühn, Niels Kuster
IT'IS Foundation, ETH Zurich, 8092 Zurich

Zurich, July, 2006

## Executive Summary

The Foundation for Research on Information Technologies in Society (IT'IS) was mandated by the Swiss Federal Office of Public Health (BAG) to perform a study on the exposure to electromagnetic fields from wireless data communication devices and to extend the frequency range of our previous work [1] up to 6 GHz.

This document provides details on the following items:

- Overview of the technologies applied in current uncontrolled wireless communication systems, i.e., wireless local networks (WLANs) employing the IEEE802.11 a/b/g/h and Bluetooth standards.

- Selection of devices with preferably the highest available radio frequency (RF) antenna output powers.

- Provision of RF and extreme low frequency (ELF) exposure components in the considered systems based on a literature review.

- Definition of worst-case operation modes and assessment procedures for incident and induced radio frequency electromagnetic fields.

- Results and evaluation of the induced and incident RF electromagnetic fields.

We analyzed short- and mid-range wireless data communication standards that are currently applied in Switzerland. Table 1 summarizes the available RF ranges and maximum regulatory permitted equivalently isotropic radiated powers of end-user devices in Switzerland as well as the maximum available net data rates of the communication systems.

| Frequency range (MHz) | Max. EIRP (mW) | Communication Standard | Max. Net Data Rate (kBit/s) |
|---|---|---|---|
| 2400 – 2483.5 | 100 | IEEE 802.11 | 1680 |
| | | IEEE 802.11b | 5940 |
| | | IEEE 802.11g | 30800 |
| | | Bluetooth | 723 |
| 5150 – 5350 | 200 | IEEE 802.11 a/h | 30800 |
| 5470 – 5725 | 1000 | IEEE 802.11a/h | 30800 |
| 880 – 915 | 2000 | GSM | 9.6 |
| | | EGPRS | 69.2 |
| 1710 – 1785 | 1000 | GSM | 9.6 |
| | | EGPRS | 69.2 |
| 1920 – 1980 | unspecified | UMTS | 2000 |

Table 1: Summary of considered frequency ranges, regulatory EIRP limits in those bands, communication standards and maximum net data rates.

For currently available WLAN standards belonging to the IEEE 802.11 family we also determined the expected ranges of extreme low frequency (ELF) and low frequency (LF) components. Because these components are generated by asynchronous burst transmission, they can vary over a wide frequency range. From the transmission of data frames the ELF components range from >0 Hz to 6.25 kHz. Additional typical ELF components result from beacon frame transmission in the range of 10 Hz.

We selected a list of devices for further experimental EMF exposure assessment as displayed in Table 2.

From the underlying communication standards we derived methods to maintain the maximum RF antenna input – i.e., the worst-case operation – during the exposure assessment.

The selected devices have been subject to incident and induced field exposure assessment. Devices with usual close-to-body application have been assessed dosimetrically according to the

| Access Points | P max (dBm) | | | | | | |
|---|---|---|---|---|---|---|---|
| | IEEE 802.11b | IEEE 802.11g | IEEE 802.11a | UMTS | GPRS 900 | GPRS 1800 | IEEE 802.15.1 |
| Netgear ProSafe WG302 | 19.8 | 19.8 | | | | | |
| ENTERASYS RBT-4102 | 20 | 20 | | | | | |
| ENTERASYS RBT-4102 | | | 20 | | | | |
| Linksys WAG55 AG | 16 | 14 | 16 | | | | |
| Cisco Aironet 1200 RB | | | 16 | | | | |
| Cisco Aironet 1200 NRB | | | 16 | | | | |
| | | | | | | | |
| **PDA** | | | | | | | |
| QTEK 9000 | unspec. | unspec. | | unspec. | 33 | 30 | unspec. |
| | | | | | | | |
| **PC cards** | | | | | | | |
| Netgear WAG511GE | 15±2 | 15±2 | 15±2 | | | | |
| Proxim ORiNOCO | 19.5 | 18 | 18 | | | | |
| 3COM XJACK | 17.5 | 19.5 | 19.5 | | | | |
| | | | | | | | |
| Belkin F5D8010 | 23.3 | 21.8 | | | | | |
| Globetrotter Fusion | 19.5 | 19.5 | | | | | |
| | | | | | | | |
| Globetrotter Fusion | | | | 24 | 33 | 30 | |

Table 2: Overview of wireless devices tested in this study. Where specified, the manufacturer-provided or distributer-provided maximum RF output powers are given.

latest draft of "Evaluation of human exposure to radio frequency fields from hand-held and body-mounted wireless communication devices in the frequency range of 30 MHz to 6 GHz" [2].

WLAN access points have been initially assessed using a novel fast pre-compliance tester or the dosimetric compliance test system, to determine the worst-case orientation with respect to the phantom surface. The final compliance tests of the WLAN access points have been conducted according to [2] in the previously determined orientation.

The incident field assessment has been conducted in a semi-anechoic chamber. The E-Fields have been be mapped in the antenna main beam direction up to a maximum distance of 2 m.

The results from the peak spatial SAR assessments are summarized in Table 4. The results from the incident E-field assessment are summarized in Table 3. The presented results do not include the measurement and DUT uncertainty. Variation of the source – e.g., source output power stability, are included in the results. Specifically, some of the WLAN devices showed insufficient source stability if used in continuous transmission mode. Therefore the worst-case source variations (power drift) were added to the results. When testing WLAN devices, it is crucial to test the device in worst-case transmission mode, i.e., with maximum transmitted unidirectional data. We optimized the data throughput by determining the connection parameters for each DUT individually. Nevertheless, some uncertainty remains due to congestion in the communication channel and non-ideal behavior of the DUT baseband communication processors, as well as drivers and operating system delays.

The tested EGPRS devices support the multi-slot class 10, i.e., they were tested with two up-link slots occupied. Devices supporting more up-link slots are rarely available. Nevertheless, a maximum of four up-link slots occupied by a single device is possible for devices supporting the multi-slot class 12.

In conclusion, all of the tested devices were compliant with European peak spatial SAR limits, i.e., 2 W/kg for the head and trunk and 4 W/kg for limbs averaged over 10 g. The PDA showed peak spatial SAR values above the 2 W/kg limit. However, the tested orientation corresponds to usage in the hand; therefore the 4 W/kg limit has to be applied.

The close margin of the exposure of these devices with respect to the safety limits emphases that compliance can only be ensured if dosimetric compliance is demonstrated, e.g., following the

procedures defined in this report. The maximum exposures within a radius of one two meters of the transmitters corresponds to typical exposures inside apartments close to base stations increasing the complexities of base station epidemiology.

| | $E_{rms}$ **(V/m)** | | | | | | | |
|---|---|---|---|---|---|---|---|---|
| | **5cm** | | **10 cm** | | **50 cm** | | **200 cm** | |
| **Communication System** | $E_{min}$ | $E_{max}$ | $E_{min}$ | $E_{max}$ | $E_{min}$ | $E_{max}$ | $E_{min}$ | $E_{max}$ |
| IEEE802.15.1 | 5.5 | | 4.0 | | 0.3 | | | |
| IEEE802.11b | 3.6 | 16.4 | 2.9 | 10.2 | 0.5 | 2.1 | 0.1 | 0.9 |
| IEEE802.11g | 1.9 | 5.0 | 1.3 | 3.1 | 0.4 | 0.6 | 0.2 | 0.3 |
| IEEE802.11a | 3.3 | 6.0 | 2.9 | 7.2 | 0.5 | 1.9 | 0.1 | 0.4 |
| EGPRS900 | 14.0 | 21.7 | 9.1 | 11.7 | 2.9 | 4.0 | 1.0 | 1.1 |
| EGPRS1800 | 10.0 | 16.4 | 7.8 | 11.6 | 1.3 | 2.3 | 0.7 | 1.1 |
| UMTS | 16.0 | 16.0 | 10.1 | 10.4 | 1.7 | 2.3 | 0.4 | 0.6 |

Table 3: Summary of the incident E-fields from wireless communication devices (Uncertainty (k=2): d≤20 cm $E_{rms}$ ±14.6% and for d>20 cm $E_{rms}$ ±31.2%).

| | peak spatial SAR (W/kg) | | | | | | | | | | | | | |
|---|---|---|---|---|---|---|---|---|---|---|---|---|---|---|
| | **IEEE 802.11b** | | **IEEE 802.11g** | | **IEEE 802.11a** | | **UMTS** | | **EGPRS 900** | | **EGPRS 1800** | | **IEEE 802.15.1** | |
| | 1g | 10g | 1g | 10g | 1g | 10g | 1g | 10g | 1g | 10g | 1g | 10g | 1g | 10g |
| **Access Points** | | | | | | | | | | | | | | |
| Netgear ProSafe WG302 | 1.00 | 0.442 | 0.55 | 0.255 | | | | | | | | | | |
| ENTERASYS RBT-4102 | 1.47 | 0.73 | 0.58 | 0.274 | | | | | | | | | | |
| ENTERASYS RBT-4102 | | | | | 0.55 | 0.180 | | | | | | | | |
| Linksys WAG55 AG | | | | | 1.86 | 0.54 | | | | | | | | |
| Cisco Aironet 1200 RB | | | | | 0.419 | 0.100 | | | | | | | | |
| Cisco Aironet 1200 NRB | | | | | 1.59 | 0.359 | | | | | | | | |
| | | | | | | | | | | | | | | |
| **PDA** | | | | | | | | | | | | | | |
| QTEK 9000 | 0.174 | 0.67 | | | | | 4.17 | 2.06 | 3.02 | 1.58 | 3.40 | 1.45 | 0.016 | 0.010 |
| | | | | | | | | | | | | | | |
| **PC cards** | | | | | | | | | | | | | | |
| Netgear WAG511GE | | | | | 0.087 | 0.050 | | | | | | | | |
| Proxim ORiNOCO | | | | | 0.106 | 0.069 | | | | | | | | |
| 3Com XJACK | | | | | 0.072 | 0.063 | | | | | | | | |
| | | | | | | | | | | | | | | |
| Belkin F5D8010 | 0.77 | 0.425 | 0.185 | 0.105 | | | | | | | | | | |
| Globetrotter Fusion | 0.220 | 0.127 | 0.110 | 0.064 | | | | | | | | | | |
| | | | | | | | | | | | | | | |
| Globetrotter Fusion | | | | | | | 0.196 | 0.123 | 0.95 | 0.67 | 0.434 | 0.284 | | |

Table 4: Summary of the peak spatial SAR results from wireless communication devices (Uncertainty (k=2): $SAR_{1g}$ ±21% / $SAR_{10g}$ ±20.5% and for IEEE802.11a(5-6 GHz) $SAR_{1g}$ ±25.9% / $SAR_{10g}$ ±25.5%).

# Contents

# 1  Introduction

Short-range wireless radio frequency (RF) devices are pervasively used in home and office environments. Currently, standards for dosimetric testing of compliance with RF electromagnetic field (EMF) safety limits for general mobile and close-to-body transmitters are under development. It is the subject of research whether measurement of the incident field strength is a reliable proxy for determining induced field strength from general mobile transmitters. Especially in scattered field zones, which have to be generally assumed in the application environment, the validity of plane wave measurement methods is questionable.

Ref. [1] shows that the strength of incident and induced fields from wireless devices in indoor environments can reach the levels of currently well perceived sources of EMF radiation, such as cellular mobile base stations and mobile telephones. Nevertheless, only little information on the expected levels of EMF exposure in the considered environments has been reported in the literature.

IT'IS was mandated by the Swiss Federal Office of Public Health (BAG) to extend their previous work on exposure in home and office environments [1] by new device classes used in the proximity of the human body as well as to extend the considered frequency range up to 6 GHz. Beside the provision of results regarding RF exposure, IT'IS was also mandated to provide information on the ranges of extreme low frequency (ELF) exposure.

The RF exposure assessment has been performed by experimental determination of induced as well as incident fields. The ELF exposure assessment has been performed by determination of possible frequency components from a review of the underlying standards.

The devices selected for the experimental exposure assessment are listed in Table 5.

| Access Points | P max (dBm) | | | | | | |
|---|---|---|---|---|---|---|---|
| | IEEE 802.11b | IEEE 802.11g | IEEE 802.11a | UMTS | GPRS 900 | GPRS 1800 | IEEE 802.15.1 |
| Netgear ProSafe WG302 | 19.8 | 19.8 | | | | | |
| ENTERASYS RBT-4102 | 20 | 20 | | | | | |
| ENTERASYS RBT-4102 | | | 20 | | | | |
| Linksys WAG55 AG | 16 | 14 | 16 | | | | |
| Cisco Aironet 1200 RB | | | 16 | | | | |
| Cisco Aironet 1200 NRB | | | 16 | | | | |
| | | | | | | | |
| **PDA** | | | | | | | |
| QTEK 9000 | unspec. | unspec. | | unspec. | 33 | 30 | unspec. |
| | | | | | | | |
| **PC cards** | | | | | | | |
| Netgear WAG511GE | 15±2 | 15±2 | 15±2 | | | | |
| Proxim ORiNOCO | 19.5 | 18 | 18 | | | | |
| 3COM XJACK | 17.5 | 19.5 | 19.5 | | | | |
| | | | | | | | |
| Belkin F5D8010 | 23.3 | 21.8 | | | | | |
| Globetrotter Fusion | 19.5 | 19.5 | | | | | |
| | | | | | | | |
| Globetrotter Fusion | | | | 24 | 33 | 30 | |

Table 5: Overview of wireless devices tested in this study. Where specified, the manufacturer-provided or distributer-provided maximum RF output powers are given.

# 2 Technologies and RF/ELF Exposure Components

## 2.1 Wireless Local Area Networks

Wireless local area networks (WLANs) in the 2.45 GHz band (IEEE 802.11b/g [3, 4, 5]) are an established source of electromagnetic radiation in Switzerland. In particular in urban areas WLANs are highly pervasive in the fields of short-range wireless data communications and are partially replacing cellular mobile communications. With upcoming standards to support roaming between different base stations (IEEE 802.11f [6]) and higher data rates (IEEE 802.11n), WLAN technology is likely to become even more pervasive and enter the realm of the traditionally centrally-operated cellular mobile systems as well as to replace wired communication channels. Due to the increasing interference in the 2.45 GHz band, the operation of WLANs in the 5-6 GHz will become more relevant in the future [7, 8]. However, 5-6 GHz applications are currently still suffering from regulatory delays, higher costs and smaller operational ranges.

Currently, in Switzerland 2.45 GHz WLAN and wireless personal area network (WPAN), e.g., Bluetooth, operation is permitted in the frequency range of 2400 to 2483.5 MHz with an equivalently isotropic radiated power (EIRP) of 100 mW [9]. In the 5 to 6 GHz band WLAN use is permitted for indoor and outdoor application in the frequency range of 5470 to 5725 MHz with an output power of 1 W with dynamic frequency selection (DFS) and transmit power control (TPC) as well as 0.5 W without transmit power control [8]. Additionally, until December 31st 2006, the band from 5150 to 5350 MHz is available for devices with an output power of 200 mW (with TPC and DFS), 120 mW (with either TPC or DFS) and 60 mW (neither DFS nor TPC) for indoor use only. From January 1st 2007 onwards the band is divided into two sub-bands ranging from 5150 to 5250 MHz and from 5250 to 5350 MHz. Both bands are licensed for indoor application only. The 5.2 GHz band is limited to 200 mW EIRP with a maximum power density of 0.25 mW/25 kHz. The 5.3 GHz band is limited to 200 mW EIRP with a maximum power density of 10 mW/MHz (with TPC) and 100 mW EIRP with a maximum power density of 5 mW/MHz (without TPC); DFS is mandatory for this band.

In addition to the currently defined frequency allocation, planning is underway for future WLANs in the frequency range from 17.1 to 17.3 GHz.

### 2.1.1 IEEE 802.11

The standard IEEE 802.11 [3] was first released in 1997 and specifies two raw data rates of 1 and 2 megabits per second (Mbit/s). It standardizes transmission via infrared (IR) signals or via an RF link in the Industrial Scientific Medical frequency band at 2.4 GHz (2.4 GHz to 2.4835 GHz). IR remains a part of the standard but has no actual implementations. The data is encoded as a spread spectrum by one of two defined spreading mechanisms; either the frequency-hopping spread spectrum (FHSS) or direct sequence spread spectrum (DSSS) and modulated on the carrier signal by 2/4 gaussian frequency shift keying (GFSK) for the FHSS and differential binary / quadrature shift keying (DBPSK / DQPSK) for DSSS. The frequency shift for GFSK is defined in the training sequence and must be greater than 110 kHz. The practical application of the legacy IEEE 802.11 is very limited.

Data transmission applying the IEEE 802.11 standard provokes a broad ELF spectrum. The lowest frequency component of access point devices is usually determined by the beacon transmission. A specific beacon interval is not mandatory; a typical value is 100 ms incorporating a 10 Hz component. In infrastructure mode WLAN network interface cards (NIC) do not transmit a beacon; however, in ad hoc mode randomly one NIC becomes responsible to manage the network and to send the beacon. Since data transmissions occur in bursts, further ELF components emerge, ranging from 0 Hz up to the minimum burst retransmission time. Access points applying the ready to send / clear to send (RTS/CTS) medium access control (MAC) extension additionally cause 36 kHz (FHSS) and 100 kHz (DSSS) components during

transmissions of remote stations. Noticeable with respect to the ELF components of FHSS is the hopping frequency of 2.5 hops per second. Additionally, it should be noted that the digital modulation processes in the IEEE 802.11 standards – i.e., all except GMSK – incorporate power envelope fluctuations. However, those are in the range of several MHz. A dynamic transmit power control is not mandatory. However, most manufacturers provide a static power control mechanism.

| RF range | (2.4 GHz to 2.4835 GHz) |
|---|---|
| max. RF $P_out$ | 100 mW |
| power control | optional (static) |
| FHSS | |
| spreading | frequency-hopping spread spectrum |
| modulation | 2 / 4 GFSK ($\Delta f > 110/2kHz$; $\Delta f > 110/4kHz$) |
| bandwidth | 79 MHz |
| hopping frequency | 2.5 Hz |
| raw data rate | 1 / 2 MBit/s |
| ELF | 0 ... 2.5 ... ~10 (beacon) ... 958 Hz |
| DSSS | |
| spreading | direct sequence spread spectrum |
| modulation | DBPSK / DQPSK |
| bandwidth | 22 MHz |
| raw data rate | 1 / 2 MBit/s |
| ELF / LF | 0 ... ~10 (beacon) ... 1.17k Hz |

### 2.1.2 IEEE 802.11b

IEEE 802.11b operates in the frequency range of 2.4 GHz to 2.4835 GHz with a channel bandwidth of 22 MHz [4]. The standard extends the legacy DSSS standard by selection of 4 (HR-5) or 64 (HR-11) spreading codes with maximized Euclidean distance from a set of $4^8$ possible spreading codes (complementary code keying (CCK)).

| RF range | (2.4 GHz to 2.4835 GHz) |
|---|---|
| max. RF $P_{out}$ | 100 mW |
| power control | optional (static) |
| HR-5.5 | |
| spreading | complementary code keying |
| modulation | DBPSK |
| bandwidth | 22 MHz |
| raw data rate | 5.5 MBit/s |
| ELF | 0 ... ~10 (beacon) ... 1.09k Hz |
| HR-11 | |
| spreading | complementary code keying |
| modulation | DQPSK |
| bandwidth | 22 MHz |
| raw data rate | 11 MBit/s |
| ELF / LF | 0 ... ~10 (beacon) ... 1.12k Hz |

### 2.1.3 IEEE 802.11g

IEEE 802.11g [5] is an extension to IEEE 802.11b in the 2.4 GHz band providing even higher data rates of up to 54 MBit/s. This is the most commonly used standard in Europe, due to high data rates and low equipment prices. The higher data rates are achieved by employing a orthogonal frequency division modulation (OFDM) for the payload data; the training sequences of the bursts stay compatible with IEEE 802.11b, i.e., spreading with CCK. Besides the maximum

rate of 54 MBit/s, transmission rates of 6, 12, 24, 36 and 48 MBit/s are available. Those rates are adaptively used if the channel quality decreases.

| RF range | (2.4 GHz to 2.4835 GHz) |
|---|---|
| max. RF $P_{out}$ | 100 mW |
| power control | optional (static) |
| spreading | CCK / OFDM |
| modulation | BPSK, QPSK, 16/64 QAM (variable coding rates) |
| bandwidth | 22 MHz |
| raw data rate | 6, 12, 24, 36 48, 54 MBit/s |
| ELF / LF | 0 ... ~10 (beacon) ... 4.42k Hz |

### 2.1.4  IEEE 802.11a/h

IEEE802.11a [7] is similar to IEEE802.11g; however it does not provide coding compatibility to IEEE802.11b. The communication system was the first to utilize the 5 to 6 GHz band on a mass-market basis.

| RF range | (5.15 GHz to 5.35 GHz / 5.725 GHz to 5.825 GHz) |
|---|---|
| max. RF $P_{out}$ | 1000 mW |
| power control | optional (static) |
| spreading | OFDM |
| modulation | BPSK, QPSK, 16/64 QAM (variable coding rates) |
| bandwidth | 22 MHz |
| raw data rate | 6, 12, 24, 36 48, 54 MBit/s |
| ELF | 0 ... ~10 (beacon) ... 4.42k Hz |

The IEEE 802.11h [8] standard is an extension to IEEE802.11a for outdoor application in the European market. The system provides transmit power control (TPC) and dynamic frequency selection (DFS). Both features were implemented by extending the beacon and NIC association frames for the TPC and a channel measurement request to support the DFS. The new beacon frame in 802.11h contains information about the geographic location, regulatory maximum power requirements, the transmit power constraint for the particular network, and a channel switch announcement section. The association frame was extended with information on the minimum power capability and supported channels of joining NICs. The channel measurement is employed to detect radars and other interferers in the communication bands.

Currently, IEEE802.11h devices are rarely available. However, with an upcoming Federal Communications Commission (FCC) regulatory act making DFS mandatory in the US, IEEE802.11h devices are expected to be more likely available in the future.

# 3  Test Modes

Testing compliance with RF exposure limits necessitates either maintaining the worst-case RF antenna input power, or having the scientific means to extrapolate to this case. In the following, the proposed test modes for the considered communication systems are presented. Additionally, maximum data throughput rates are provided in order to normalize the subsequently determined SAR results, i.e, to $SAR/kBps$ for the individual communication systems as proposed by BAG.

## 3.1  WLAN

In general, the maximum output power for WLAN systems can be achieved by maintaining the maximum time-averaged data throughput. In IEEE 802.11 each transmitter station congests for the channel. The channel congestion can be minimized if only a single station requests transmission at a time. Therefore the obvious way to test is to establish a unidirectional data transmission from the device under test (DUT) to another receiving station. In this study this was achieved by setting up a User Datagram Protocol (UDP) data stream from the DUT to the remote station.

As shown in [10] the theoretical maximum throughput can be achieved by an infinite sized medium access control (MAC) service data unit (SDU), i.e., the protocol overhead becomes negligible relative to the transmitted payload data. However, in real networks the maximum MSDU size is usually limited to 1500 Bytes; larger MSDU are fragmented into smaller packages. Considering the Internet protocol (IP) and (UDP) headers of 20+8 Bytes, the maximum throughput can be achieved with a UDP payload of 1472 Byte.

With a unidirectional transmission established, further transmission timeouts are only due to the channel access mechanism and acknowledge transmissions. In IEEE 802.11 two different channel access mechanisms can be employed; carrier sense multiple access with collision avoidance (CSMA/CA), and CSMA/CA with ready to send / clear to send (RTS/CTS) extension. If the RTS/CTS extension is used, the crest factor is generally higher than for CSMA/CA only; therefore, for compliance testing the CSMA/CA mechanism is preferred.

For example to achieve the worst-case operational mode of an IEEE 802.11b device we propose using a UDP transmission with 1472 byte payload and the access mode with the lowest crest factor. A contention window size of half of the maximum size was chosen. For High-Rate-CCK-11 with CSMA/CA the crest factor is:

$$cf_{CSMA/CA} = \frac{674 + 8/11 \cdot (34 + MSDU)}{309 + 8/11 \cdot (34 + MSDU)} \cdot \frac{\mu s}{\mu s} \tag{1}$$

It is obvious that the crest factor is affected by the size of the MSDU (in bytes). In our case with a MSDU of $1472 + 20 + 8$ bytes ($20 + 8$ accounts for the IP/UDP header) the crest factor is 1.52.

If the RTS/CTS MAC-extension is applied, the crest factor is:

$$cf_{RTS/CTS} = \frac{1331 + 8/11 \cdot (34 + MSDU)}{661 + 8/11 \cdot \cdot (34 + MSDU)} \cdot \frac{\mu s}{\mu s} \tag{2}$$

A 1500 Byte MSDU payload gives a crest factor of 2.03.

The testing will be performed with the device operating at channels 1, 7 and 13 in order to cover frequency dependencies over the band.

In the following we summarize the theoretical minimum crest factors and maximum data rates (at 1472 Bytes UDP payload per MSDU) for the considered IEEE 802.11 system to establish a worst-case connection during testing.

### 3.1.1  IEEE 802.11

|         |        | min. crest factor | max. data rate (Bit/s) |
|---------|--------|-------------------|------------------------|
| **CSMA/CA** | FHSS-1 | 1.06 | 870k |
|         | FHSS-2 | 1.12 | 1.63M |
|         | DSSS-1 | 1.05 | 896k |
|         | DSSS-2 | 1.11 | 1.68M |
| **RTS/CTS** | FHSS-1 | 1.11 | 833k |
|         | FHSS-2 | 1.21 | 1.51M |
|         | DSSS-1 | 1.11 | 853k |
|         | DSSS-2 | 1.21 | 1.53M |

Dynamic power control is not implemented; optional static power control must be set to maximum power.

### 3.1.2  IEEE 802.11b

|         |        | min. crest factor | max. data rate (Bit/s) |
|---------|--------|-------------------|------------------------|
| **CSMA/CA** | HR-5.5 | 1.28 | 3.80M |
|         | HR-11  | 1.51 | 5.94M |
| **RTS/CTS** | HR-5.5 | 1.56 | 3.12M |
|         | HR-11  | 2.03 | 4.43M |

Dynamic power control is not implemented; optional static power control must be set to maximum power.

### 3.1.3  IEEE 802.11g/a

|         |         | min. crest factor | max. data rate (Bit/s) |
|---------|---------|-------------------|------------------------|
| **CSMA/CA** | OFDM-54 | 1.54 | 30.8M |
| **RTS/CTS** | OFDM-54 | 1.81 | 26.3M |

Dependent on the channel quality, the system adjusts the data rate of each sub-carrier separately, i.e., the actual maximum data rate can further decrease. Dynamic power control is not implemented; optional static power control must be set to maximum power.

## 3.2  Bluetooth

The output power of a Bluetooth device can be influenced in two ways: 1) by the time division duplex method and 2) by the power control.

During a compliance test it is necessary for the receiver to request the maximum output power from the DUT. Bluetooth power class I devices have a power control limiting the transmitted power over $0\,$dBm. A power control for class II and III devices is optional. The power control is based on signal strength detection at the receiver. This information is sent to the transmitter by the Receiver Signal Strength Indicator (RSSI).

If the highest peak output power is set by the power control, the time-averaged output power depends only on the DUT's duty cycle. Therefore, it is necessary to operate the DUT with the lowest applicable crest factor. Theoretically, the lowest crest factor can be achieved if a device (Master) continuously transmits 5-slot bursts interrupted by one slot reserved for the remote device (Slave).

$$cf_{min} = \frac{3750\,\mu s}{2871\,\mu s} = 1.3 \tag{3}$$

However, Bluetooth provides a wide range of application dependent communication profiles that may not utilize multi-slot transmission. Thus, under more realistic conditions the crest factor is larger due to single-slot transmissions, shorter bursts and interleaved slots.

For sound compliance tests we recommend setting the DUT into a well defined transmission mode and extrapolating to the worst-case situation. This mode is best achieved by setting the DUT into the Bluetooth test mode and subsequently performing a transmitter test [11]. The DUT may only be set into the test mode by manufacturer-provided software or hardware tools. Additionally, a Bluetooth tester is necessary to perform the tests. The recommended parameters for the transmitter test according to [11] are summarized in Table 6.

| Parameter | Setting |
|---|---|
| Test Scenario | 3 (transmitter test - 1010 pattern) |
| Hopping Mode | 1 / 3 (hopping Europe, USA / France) |
| Power Control Mode | 1 (adaptive power control) |
| Poll Period | 1 (1.25 ms) |
| Packet type | 0111 (HV3) |
| Length of test sequence | 30 (240 bit payload) |

Table 6: Recommended setting for Bluetooth Link Manager Protocol (LMP) Test Control PDU

In this configuration the DUT transmits for 366 $\mu s$ in every second slot. The Bluetooth specification is unclear about the actual output power if fixed output power is used in the test mode. The DUT is therefore operated using adaptive power control. According to [11] the normal link manager protocol commands for power control can be used to request maximum output power. An E-field ($E_{test}$) measured in this mode can be extrapolated to the maximum possible E-field for 5-slot transmissions ($E_{max}$):

$$\langle E_{max}\rangle_t = \sqrt{\frac{2871}{1098}}\,\langle E_{test}\rangle_t \tag{4}$$

## 3.3  Cellular Mobile Systems

All considered cellular mobile systems systems can be forced to maximum output power using a base station emulator, e.g., the CMU200 from Rohde & Schwarz (Germany). The DUT is connected to the tester, and the maximum output power is requested via transmit power control parameters from the DUT. For Enhanced General Packet Radio Service (EGPRS) it is necessary to test the DUT with maximum possible slot usage. The selected EGPRS devices support the multi-slot class 10, i.e., they were tested with two up-link slots occupied. Devices supporting more up-link slots are rarely available. Nevertheless, a maximum of four up-link slots occupied by a single device is possible for devices supporting the multi-slot class 12. For mobile stations employing the Universal Mobile Telecommunications System (UMTS) it is further necessary to set the DUT in loop-back mode and to transmit random data at full vocoder rate for voice application and full rate for data applications. However, it is assumed that this has a negligible effect on the average output power using the UMTS communication system. The maximum data rates of these systems are summarized in Table 7.

| System | max. data rate (kBps) |
|---|---|
| GSM | 9.6 (per slot) |
| EGPRS | 69.2 (per slot) |
| UMTS | 2000 |

Table 7: Maximum data rates of European cellular mobile communication systems.

# 4   Dosimetric Exposure Assessment

## 4.1   3-D Scanning System

At high frequencies, measurements must be made in several hundreds of points with high field ($<10\ \mu$W/g) and spatial precision ($< 0.2\ mm$), to achieve low measurement uncertainty in view of the high attenuation and large spatial field variations within the tissue emulation liquid. To obtain results of the greatest reliability the dosimetric assessment system DASY4, SPEAG (Figure 1) has been employed. The specifications of the system are summarized in Table 8.



Figure 1: DASY 4 dosimetric assessment system (SPEAG)

### 4.1.1   Probe Requirements

The strong field gradients inside tissue simulating materials at higher frequencies require smaller tip diameter, measurements much closer to the surface and graded measurement grids. In cooperation with SPEAG, we developed the smallest 3-sensor probe EX3DV3 (Figure 2), the performance of which is summarized in Table 9. The calibration methods as well as the scanning procedures have been adopted to facilitate the most accurate measurements, even for frequencies up to 6 GHz. The performance is consistent with the requirements of Annex B of [2].

### 4.1.2   Dosimetric Phantom

Dosimetric assessments for close-to-body and general mobile transmitters require phantoms that emulate the properties of typical application positions and that provide good reproducibility as well as worst-case exposure conditions. The standard draft IEC 62209 "Evaluation of human exposure to radio frequency fields from hand-held and body-mounted wireless communication devices in the frequency range of 30 MHz to 6 GHz" suggests a liquid filled flat phantom of the elliptical dimensions 600mm by 400mm [2].

| **System** | Type: | DASY4 Professional |
| | Software: | DASY4, V4.4 Build3; SEMCAD, V1.8 Build 1.30 |
| **Positioner** | Robot: | RX90L |
| | Serial Number: | F99/5A80A1/A/02 |
| | Range: | 1185 mm |
| | Repeatability: | ±0.025 mm |
| | Controller: | CS7MB |
| | Serial Number: | F99/5A80A1/A/02 |
| | Manufacturer: | Stäubli France |
| **Data Acquisition System** | Type: | DAE3V.1 |
| | Serial No: | 355 |
| | Calibrated On: | May 2005 |
| | Manufacturer: | Schmid & Partner Engineering AG (CH) |

Table 8: Specifications: DASY4 dosimetric assessment system



Figure 2: Novel miniature isotropic dosimetric field probe (EX3DV3, SPEAG).

| Type: | EX3DV3 |
| --- | --- |
| Serial | 3515 |
| Frequency Range: | 30 MHz to 6 GHz |
| Dynamic Range: | 10 $\mu$W/g to 100 mW/g |
| Spherical Isotropy: | < ±0.5 dB |
| Boundary Effect: | error at 0.5 mm distance: 3 % |
| | no error (< 0.1 dB) at: 2 mm |
| Dimensions: | dipole length: 2.1 mm |
| | dipole offset: 1.0 mm |
| | tip diameter: 2.5 mm (incl. cover) |

Table 9: Specifications: Miniature isotropic dosimetric field probe.

In accordance with [2] the assessments were conducted with the ELI4 phantom from SPEAG, Switzerland, specified in Table 10 (Figure 3). This phantom has been extensively characterized for the application in the frequency range from 30 MHz to 6 GHz [12].
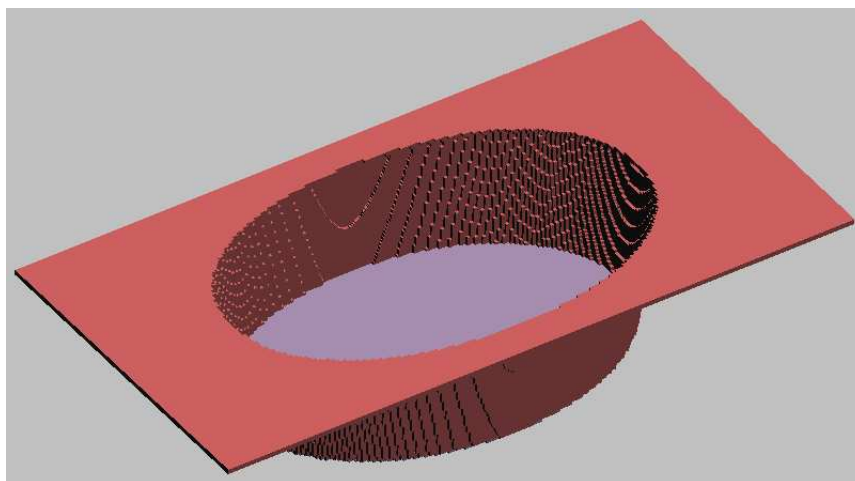


Figure 3: Elliptical Phantom CAD model.

| Type | ELI4 |
|---|---|
| Serial | 1010 |
| Bottom Thickness: | 2.0 ± 0.2 mm (sagging: <1%) |
| Filling Volume: | approx. 30 liters |
| Dimensions: | Major ellipse axis: 600 mm |
| | Minor axis: 400 mm |

Table 10: Specifications: ELI4 phantom for body-mounted and body-supported devices.

### 4.1.3 Tissue Emulating Liquids

The tissue equivalent liquid parameters have been chosen according to [2]. The target liquid dielectric parameters are summarized in Table 11; the table is extended by liquid parameters at the low, middle, high frequencies of the considered bands by linear extrapolation.

### 4.1.4 Assessment Procedures Using DASY4

In advance of any dosimetric assessment, a system performance check is conducted which verifies the correct functionality of the measurement system.

This is done by the application of a known power level to a well defined RF EMF source (calibration dipole). Then a measurement in accordance with the procedure described below is performed, and the measured SAR values are compared to the target values in the dipole calibration certificate, or to [2].

The measurement procedure implements the protocol of clause 6.3 of [2].

- **Step 1:** Measurement of the SAR value at a fixed location within 10 mm of the inner surface of the phantom is used as a reference value for assessing the power drop.

- **Step 2:** The SAR distribution within the phantom is measured at a distance of 4.0 mm from the inner surface of the shell. The scan covers the area of the DUT projected on the phantom surface, and the horizontal grid spacing is 15 mm x 15 mm. Based on this data, the location of maximum absorption is determined by using the Quadratic Shepard's method [13].

| Frequency MHz | Real part of the complex relative permittivity, $\epsilon'_r$ | Conductivity, $\sigma$ (S/m) |
|---|---|---|
| 30 | 55.0 | 0.75 |
| 150 | 52.3 | 0.76 |
| 300 | 45.3 | 0.87 |
| 450 | 43.5 | 0.87 |
| 835 | 41.5 | 0.90 |
| 900 | 41.5 | 0.97 |
| 1450 | 40.5 | 1.20 |
| 1800 | 40.0 | 1.40 |
| 1900 | 40.0 | 1.40 |
| 2000 | 40.0 | 1.40 |
| **2400** | **39.3** | **1.76** |
| **2450** | **39.2** | **1.80** |
| **2500** | **39.1** | **1.85** |
| 3000 | 38.5 | 2.40 |
| 4000 | 38.0 | 3.50 |
| 5000 | 36.2 | 4.40 |
| **5150** | **36.1** | **4.63** |
| 5200 | 36.0 | 4.70 |
| **5250** | **36.0** | **4.75** |
| **5350** | **35.9** | **4.85** |
| 5400 | 35.8 | 4.90 |
| **5500** | **35.7** | **4.97** |
| **5600** | **35.6** | **5.03** |
| **5700** | **35.6** | **5.10** |
| 6000 | 35.3 | 5.30 |

Table 11: Dielectric parameters of the liquid material (extended by liquid parameters at the low, mid and high frequencies (bold) of the considered bands by linear interpolation.

- **Step 3:** Around this point and all sub-maxima within a threshold of 2 dB, a volume is assessed in accordance to the requirement of [2]. The evaluation of the spatial peak SAR values is performed within the post-processing of the measured data [13]. For determining the cube with the highest average SAR, the following algorithm is implemented:

  - extraction of the measured data from the performed volume scan (grid and values)
  - calculation of the SAR at each measured point
  - generation of high-resolution mesh within the measured volume
  - interpolation of the measured values from the measured grid to the high-resolution grid by using a combination of a least-square fitted function method and a weighted average method
  - extrapolation of the entire 3-D field distribution to the phantom surface over the distance from sensor to surface
  - calculation of the averaged SAR over the masses of 1 g and 10 g

- **Step 4:** Re-measurement of the SAR value at the same location as in Step 1 in order to determine any power difference.

This procedure needs to be repeated for all configurations in order to assess the worst-case exposure. The time required for identifying the worst-case configuration can be greatly reduced if fast scanners are employed.

## 4.2 Fast Planar Array Scanner (Preliminary Evaluation)

The scanner (iSAR from SPEAG) is based on a sensor array implanted in a solid flat phantom (Figure 4). The phantom is filled with a broadband tissue simulating gel (300 MHz to 6 GHz), with sensors located at 4 mm below the surface. The density of the sensor array (15 mm) is sufficient to reliably assess the exposure. The measured SAR values of all sensors are acquired and integrated in parallel, such that the total assessment time is less than 3 seconds. The scanner has been used to support preliminary evaluations of WLAN access points.
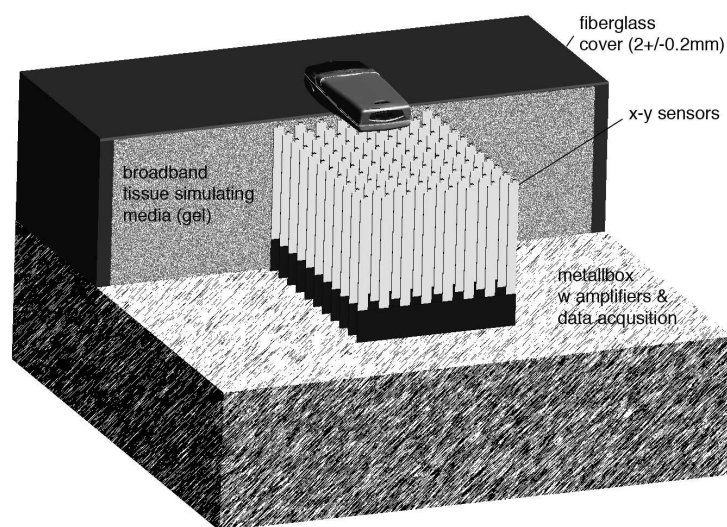


Figure 4: The concept of a fast dosimetric scanner (iSAR, SPEAG), based on a dense array of sensors completely immersed in a broadband tissue simulating medium. In order to provide quick response and to increase the signal-to-noise ratio, the signals of all sensors must be amplified and integrated in parallel. The high-resistive sensor leads are vertical to minimize field distortions.

# 5   Applied Evaluation Procedures

## 5.1   Assessment Procedure for Body-Mounted, Body-Supported Devices

The assessment of WLAN PC cards and the PDA device have been performed according to the latest draft of "Evaluation of human exposure to radio frequency fields from hand-held and body-mounted wireless communication devices in the frequency range of 30 MHz to 6 GHz":

- WLAN-equipped portable personal computers were positioned at the phantom, as if the phantom represented the users lap (Figure 5). The screen was tested at a 90° angle to the phantom bottom. For devices with possible radiators in the display section, an angle with the display as close as possible to the phantom was tested in addition to the requirements of [2].

- The selected PDA device can be used "laptop-like"; therefore it has also been tested according to Figure 5. Additionally, it has been tested with the screen section covering the alpha-numerical keypad and attached to the phantom with its back side as displayed in Figure 6.
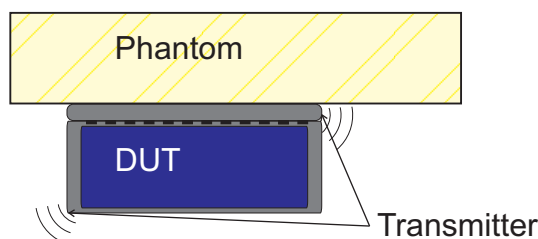


Figure 5: A body-supported device attached to the dosimetric measurement phantom.
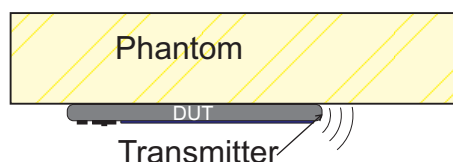


Figure 6: A hand-held attached to the dosimetric measurement phantom.

## 5.2   Assessment Procedure for WLAN Access Points

The WLAN access point devices have been tested with worst-case positioning attached to the ELI4 phantom. The assessment has been conducted according to the following procedure:

- **Step 1:** Systematic evaluation of independent orientations of the DUT relative to the phantom surface using the iSAR fast dosimetric scanner (see Section 4.2) or the DASY4 system.

- **Step 2:** Determination of the worst-case absorbing position from the preliminary evaluation.

- **Step 3:** Assessment of the spatial peak SAR using the 3-D scanner with the DUT attached to the phantom in the worst-case orientation (Figure 7).
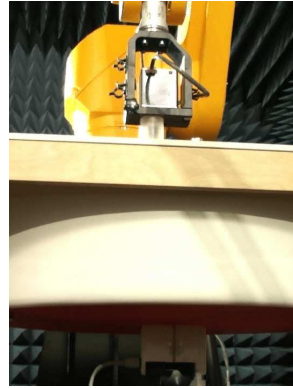
Figure 7: A WLAN access point attached to the ELI4 phantom.

## 6   Uncertainty Budget of the Dosimetric Evaluation

The dosimetric measurement uncertainties in accordance with IEC 62209 part 2 up to 3 GHz are displayed in Table 12. The uncertainty budget for dosimetric compliance testing in the frequency range between 5 to 6 GHz is given in Table 13.

| DASY4 Uncertainty Budget<br>According to IEC 62209 [2] | | | | | | | | |
|---|---|---|---|---|---|---|---|---|
| Error Description | Uncertainty<br>value | Prob.<br>Dist. | Div. | $(c_i)$<br>1g | $(c_i)$<br>10g | Std. Unc.<br>(1g) | Std. Unc.<br>(10g) | $(v_i)$<br>$v_{eff}$ |
| **Measurement System** | | | | | | | | |
| Probe Calibration | ±5.9 % | N | 1 | 1 | 1 | ±5.9 % | ±5.9 % | ∞ |
| Axial Isotropy | ±4.7 % | R | $\sqrt{3}$ | 0.7 | 0.7 | ±1.9 % | ±1.9 % | ∞ |
| Spherical Isotropy | ±9.6 % | R | $\sqrt{3}$ | 0.7 | 0.7 | ±3.9 % | ±3.9 % | ∞ |
| Boundary Effects | ±1.0 % | R | $\sqrt{3}$ | 1 | 1 | ±0.6 % | ±0.6 % | ∞ |
| Linearity | ±4.7 % | R | $\sqrt{3}$ | 1 | 1 | ±2.7 % | ±2.7 % | ∞ |
| Detection Limits | ±1.0 % | R | $\sqrt{3}$ | 1 | 1 | ±0.6 % | ±0.6 % | ∞ |
| Readout Electronics | ±0.3 % | N | 1 | 1 | 1 | ±0.3 % | ±0.3 % | ∞ |
| Response Time | ±0.8 % | R | $\sqrt{3}$ | 1 | 1 | ±0.5 % | ±0.5 % | ∞ |
| Integration Time | ±2.6 % | R | $\sqrt{3}$ | 1 | 1 | ±1.5 % | ±1.5 % | ∞ |
| Perturbation of the Environment | ±3.0 % | R | $\sqrt{3}$ | 1 | 1 | ±1.7 % | ±1.7 % | ∞ |
| Probe Positioner Mech. Restr. | ±0.4 % | R | $\sqrt{3}$ | 1 | 1 | ±0.2 % | ±0.2 % | ∞ |
| Probe Positioning | ±2.9 % | R | $\sqrt{3}$ | 1 | 1 | ±1.7 % | ±1.7 % | ∞ |
| Post-Processing | ±1.0 % | R | $\sqrt{3}$ | 1 | 1 | ±0.6 % | ±0.6 % | ∞ |
| **Test Sample Related** | | | | | | | | |
| Test Sample Positioning | ±2.9 % | N | 1 | 1 | 1 | ±2.9 % | ±2.9,% | 145 |
| Device Holder Uncertainty | ±3.6 % | N | 1 | 1 | 1 | ±3.6 % | ±3.6 % | 5 |
| Drift of Output Power | ±5.0 % | R | $\sqrt{3}$ | 1 | 1 | ±2.9 % | ±2.9 % | ∞ |
| **Phantom and Setup** | | | | | | | | |
| Phantom Uncertainty | ±4.0 % | R | $\sqrt{3}$ | 1 | 1 | ±2.3 % | ±2.3 % | ∞ |
| Liquid Conductivity (target) | ±5.0 % | R | $\sqrt{3}$ | 0.7 | 0.5 | ±2.0 % | ±1.4 % | ∞ |
| Liquid Conductivity (meas.) | ±4.3 % | R | $\sqrt{3}$ | 0.7 | 0.5 | ±1.7,% | ±1.2 % | ∞ |
| Liquid Permittivity (target) | ±5.0 % | R | $\sqrt{3}$ | 0.6 | 0.5 | ±1.7 % | ±1.4 % | ∞ |
| Liquid Permittivity (meas.) | ±4.3 % | R | $\sqrt{3}$ | 0.6 | 0.5 | ±1.5 % | ±1.2 % | ∞ |
| Combined Std. Uncertainty | | | | | | ±10.5 % | ±10.2 % | 330 |
| **Expanded Uncertainty** | | | | | | **±21.0 %** | **±20.5 %** | |

Table 12: Worst-Case uncertainty budget for DASY4 assessed according to IEC 62209 [2]. The budget is valid for the frequency range 300 MHz - 3 GHz and represents a worst-case analysis. For specific tests and configurations, the uncertainty could be considerable smaller.

| **DASY4 Uncertainty Budget** | | | | | | | | |
|---|---|---|---|---|---|---|---|---|
| **for the 5 - 6 GHz range** | | | | | | | | |
| Error Description | Uncertainty value | Prob. Dist. | Div. | $(c_i)$ 1g | $(c_i)$ 10g | Std. Unc. (1g) | Std. Unc. (10g) | $(v_i)$ $v_{eff}$ |
| **Measurement System** | | | | | | | | |
| Probe Calibration | ±6.8 % | N | 1 | 1 | 1 | ±6.8 % | ±6.8 % | ∞ |
| Axial Isotropy | ±4.7 % | R | $\sqrt{3}$ | 0.7 | 0.7 | ±1.9 % | ±1.9 % | ∞ |
| Hemispherical Isotropy | ±9.6 % | R | $\sqrt{3}$ | 0.7 | 0.7 | ±3.9 % | ±3.9 % | ∞ |
| Boundary Effects | ±2.0 % | R | $\sqrt{3}$ | 1 | 1 | ±1.2 % | ±1.2 % | ∞ |
| Linearity | ±4.7 % | R | $\sqrt{3}$ | 1 | 1 | ±2.7 % | ±2.7 % | ∞ |
| System Detection Limits | ±1.0 % | R | $\sqrt{3}$ | 1 | 1 | ±0.6 % | ±0.6 % | ∞ |
| Readout Electronics | ±0.3 % | N | 1 | 1 | 1 | ±0.3 % | ±0.3 % | ∞ |
| Response Time | ±0.8 % | R | $\sqrt{3}$ | 1 | 1 | ±0.5 % | ±0.5 % | ∞ |
| Integration Time | ±2.6 % | R | $\sqrt{3}$ | 1 | 1 | ±1.5 % | ±1.5 % | ∞ |
| RF Ambient Noise | ±3.0 % | R | $\sqrt{3}$ | 1 | 1 | ±1.7 % | ±1.7 % | ∞ |
| RF Ambient Reflections | ±3.0 % | R | $\sqrt{3}$ | 1 | 1 | ±1.7 % | ±1.7 % | ∞ |
| Probe Positioner | ±0.8 % | R | $\sqrt{3}$ | 1 | 1 | ±0.5 % | ±0.5 % | ∞ |
| Probe Positioning | ±9.9 % | R | $\sqrt{3}$ | 1 | 1 | ±5.7 % | ±5.7 % | ∞ |
| Max. SAR Eval. | ±4.0 % | R | $\sqrt{3}$ | 1 | 1 | ±2.3 % | ±2.3 % | ∞ |
| **Test Sample Related** | | | | | | | | |
| Device Positioning | ±2.9 % | N | 1 | 1 | 1 | ±2.9 % | ±2.9 % | 145 |
| Device Holder | ±3.6 % | N | 1 | 1 | 1 | ±3.6 % | ±3.6 % | 5 |
| Power Drift | ±5.0 % | R | $\sqrt{3}$ | 1 | 1 | ±2.9 % | ±2.9 % | ∞ |
| **Phantom and Setup** | | | | | | | | |
| Phantom Uncertainty | ±4.0 % | R | $\sqrt{3}$ | 1 | 1 | ±2.3 % | ±2.3 % | ∞ |
| Liquid Conductivity (target) | ±5.0 % | R | $\sqrt{3}$ | 0.64 | 0.43 | ±1.8 % | ±1.2 % | ∞ |
| Liquid Conductivity (meas.) | ±2.5 % | N | 1 | 0.64 | 0.43 | ±1.6 % | ±1.1 % | ∞ |
| Liquid Permittivity (target) | ±5.0 % | R | $\sqrt{3}$ | 0.6 | 0.49 | ±1.7 % | ±1.4 % | ∞ |
| Liquid Permittivity (meas.) | ±2.5 % | N | 1 | 0.6 | 0.49 | ±1.5 % | ±1.2 % | ∞ |
| Combined Std. Uncertainty | | | | | | ±12.9 % | ±12.7 % | 330 |
| **Coverage Factor for 95%** | | **kp=2** | | | | | | |
| **Expanded STD Uncertainty** | | | | | | **±25.9 %** | **±25.5 %** | |

Table 13: Worst-Case uncertainty budget for DASY4 valid for the frequency range 5 - 6 GHz. Probe calibration error reflects uncertainty of the narrow-bandwidth EX3DVx probe conversion factor (±50 MHz).

# 7   Incident E-Field Assessment

## 7.1   Positioner System

The free-space measurements have been assisted by a robot positioner. The specifications of the positioner system are given in Section 4.1.

## 7.2   Near Field Probes

Miniature free space E/H-field probes have been applied to assess the incident E/H-field exposure at closest distances to the transmitters. The probe specifications are summarized in Table 14.

| **E-Field Probe** | Type: | ER3DV6 |
|---|---|---|
| | Serial Number: | 2335 |
| | Manufacturer: | Schmid & Partner Engineering AG (CH) |
| | Calibrated on: | January 2005 |
| | Tip Diameter: | 8 mm |
| | Frequency Range: | 100 to 10000 MHz |
| | Dynamic Range: | $2\,V/m$ to $\geq 1000\,V/m$ |
| | Dev. Axial Isotropy: | $\leq \pm 0.2\,dB$ (30 to 2500 MHz) |
| | Dev. Spherical Isotropy: | $\leq \pm 0.4\,dB$ |
| | Calibration Uncertainty: | $\pm 6.0\%$ (k=2) |
| **H-Field Probe** | Type: | H3DV6 |
| | Serial Number: | 6065 / 6060 |
| | Manufacturer: | Schmid & Partner Engineering AG (CH) |
| | Calibrated on: | January 2005 / August 2004 |
| | Tip Diameter: | 6 mm |
| | Frequency Range: | 200 to 3000 MHz |
| | Dynamic Range: | $2\,mA/m$ to $2\,A/m$ at 1 GHz |
| | Dev. Spherical Isotropy: | $\leq \pm 0.25\,dB$ |
| | Calibration Uncertainty: | $\pm 6.0\%$ (k=2) |

Table 14: Specifications: E/H-field probes for near field incident field assessments.

## 7.3   Far Field Incident Field Measurement Equipment

Due to limited sensitivity of the near field probes, the E-Field assessment in the far field zone of the transmitter has been performed using a ARCS PCD8250 conical dipole antenna (Seibersdorf Research, Austria) for measurements up to 2.5 GHz. For the 5-6 GHz range a double ridge horn antenna was used. A Rohde & Schwarz FSP30 spectrum analyzer was used as the measurement receiver. The specifications of the far field measurement equipment are summarized in Table 15.

The spectrum analyzer detector type, sweep time and filter bandwidth settings have been optimized by transfer calibration from a thermal power meter measurement for the individual signal types.

## 7.4   Assessment Procedure

The worst-case incident field distributions have been assessed according to the following steps:

- **Step 1:** Determination of the E-field maximum from three mutually orthogonal 360° rotations of the DUT (see Figure 8).

- **Step 2:** Mapping of the incident near field E and H-fields (H-field for 2.5 GHz devices only) in the direction of the previously determined maximum (up to 20 cm or to probe sensitivity limit).

| Spectrum Analyzer | Type: | Rohde & Schwarz FSP 9 kHz...30 GHz |
|---|---|---|
| | Software: | Firmware V1.20 |
| | Manufacturer: | Rohde & Schwarz (D) |
| | Frequency Range | 9 kHz...30 GHz |
| Attenuator | Type: | VAT-10 |
| | Manufacturer: | Mini Circuits (USA) |
| Cable | Type: | RG142 |
| | Serial No: | K171/02 |
| | Calibrated on: | April 2002 |
| | Manufacturer: | ARC Seibersdorf (A) |
| Antennas | Type: | PCD 8250 |
| | Serial Number: | 3158/02 |
| | Calibrated on: | April 2002 |
| | Manufacturer: | ARC Seibersdorf (A) |
| | Frequency Range | 80 MHz...2.5 GHz |

Table 15: Specifications: Far field measurement system

- **Step 3:** Mapping of the incident far field E-fields in the direction of the previously determined maximum (up to 200 cm)
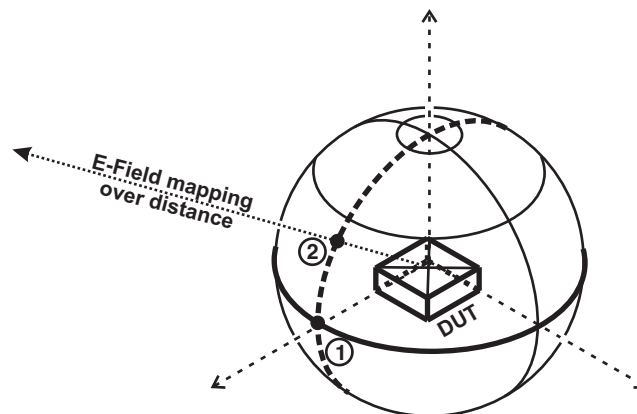


Figure 8: Directivity assessment of the DUT along two perpendicular great circles with determined maxima (1) and (2)

## 7.5 Uncertainty

In contrast to the previous study [1] the incident field assessments have been supported by a robot positioner. Therefore, the uncertainty of the incident field assessment decreases as displayed in Tables 16 and 17.

## 7.6 Source Variations

Uncontrolled applicable communication systems such as IEEE802.11x do not include sound test modes like UMTS or EGPRS. Hence, especially for those devices, a higher uncertainty due to source variation has to be expected. We suggest that establishing the highest unidirectional data transmission rate results in the highest time-averaged output power. However, there are factors that should be considered as variations when testing under this assumption:

- Data rate dependent output powers (IEEE802.11a/g devices usually have different nominal output power for different channel rates)

| Error Description | Uncertainty value $\pm$ % | Probability distribution | Divisor | $(c_i)$ | Std. unc. | $(v_i)^2$ or $v_{eff}$ |
|---|---|---|---|---|---|---|
| **Measurement Equipment** | | | | | | |
| Probe calibration | $\pm 2.0\,\%$ | normal | 1 | 1 | $\pm 3.0\,\%$ | $\infty$ |
| Axial isotropy of the probe | $\pm 4.5\,\%$ | rectang. | $\sqrt{3}$ | 1 | $\pm 2.6\,\%$ | $\infty$ |
| Spherical isotropy of the probe | $\pm 9.6\,\%$ | rectang. | $\sqrt{3}$ | 0.7 | $\pm 3.9\,\%$ | $\infty$ |
| Probe linearity | $\pm 4.7\,\%$ | rectang. | $\sqrt{3}$ | 1 | $\pm 2.7\,\%$ | $\infty$ |
| Readout electronics | $\pm 1.0\,\%$ | normal | 1 | 1 | $\pm 1.0\,\%$ | $\infty$ |
| Integration time | $\pm 2.6\,\%$ | rectang. | $\sqrt{3}$ | 1 | $\pm 1.5\,\%$ | $\infty$ |
| Response time | $\pm 0.8\,\%$ | rectang. | $\sqrt{3}$ | 1 | $\pm 0.5\,\%$ | $\infty$ |
| **Setup** | | | | | | |
| Probe Positioning | $\pm 6.0\,\%$ | rectang. | $\sqrt{3}$ | 1 | $\pm 3.5\,\%$ | $\infty$ |
| Power Drift | $\pm 5.0\,\%$ | rectang. | $\sqrt{3}$ | 1 | $\pm 0.6\,\%$ | $\infty$ |
| RF Ambient Conditions | $\pm 3.0\,\%$ | rectang. | $\sqrt{3}$ | 1 | $\pm 1.7\,\%$ | $\infty$ |
| Combined Std. Uncertainty | | | | | $\pm \mathbf{7.3\,\%}$ | |
| **Coverage Factor for 95%** | | **kp=2** | | | | |
| **Expanded Std. Uncertainty** | | | | | $\pm \mathbf{14.6\,\%}$ | |

Table 16: Uncertainty budget of the near field measurements.

| Error Description | Uncertainty value $\pm$ % | Probability distribution | Divisor | $(c_i)$ | Std. unc. | $(v_i)^2$ or $v_{eff}$ |
|---|---|---|---|---|---|---|
| **Measurement Equipment** | | | | | | |
| Antenna Factor Cal. | $\pm 25.9\,\%$ | normal (k=2) | 2 | 1 | $\pm 13\,\%$ | $\infty$ |
| Cable Loss Cal. | $\pm 1.8\,\%$ | normal (k=2) | 2 | 1 | $\pm 0.9\,\%$ | $\infty$ |
| Attenuator Cal. | $\pm 7.2\,\%$ | rectang. | $\sqrt{3}$ | 1 | $\pm 4.2\,\%$ | $\infty$ |
| Receiver Spec. | $\pm 6.4\,\%$ | normal (k=2) | 2 | 1 | $\pm 3.2\,\%$ | $\infty$ |
| Mismatch | $\pm 9.4\,\%$ | rectang. | $\sqrt{2}$ | 1 | $\pm 6.6\,\%$ | $\infty$ |
| **Setup** | | | | | | |
| Antenna Positioning | $\pm 2.0\,\%$ | rectang. | $\sqrt{3}$ | 1 | $\pm 1.2\,\%$ | $\infty$ |
| Power Drift | $\pm 5.0\,\%$ | rectang. | $\sqrt{3}$ | 1 | $\pm 0.6\,\%$ | $\infty$ |
| Combined Std. Uncertainty | | | | | $\pm \mathbf{15.6\,\%}$ | |
| **Coverage Factor for 95%** | | **kp=2** | | | | |
| **Expanded Std. Uncertainty** | | | | | $\pm \mathbf{31.2\,\%}$ | |

Table 17: Uncertainty budget of the far field measurement setups.

- Multiple input multiple output, spatial diversity antennas (application of those can change the radiation pattern of the DUT during the tests)

- DUT baseband communication processors (baseband processing has influence on the communication rate)

- Channel congestion (remote station can congest for the channel with the DUT)

- Medium access control fragmentation (packet fragmentation size can be less than the maximum of 1500 Bytes)

- Software of the DUT and Remote PC (delays in drivers and operating systems influence the data rate)

The variations due to the factors listed are hardly enough to assess for a DUT individually since they can only be approached by statistical means. In summary, the uncertainty due to the source variations of IEEE802.11x devices can easily exceed a factor of 3 dB.

# 8 Results

## 8.1 Validation of the SAR Measurement System

In advance of the actual DUT compliance tests, system validation measurements with reference dipoles and known input power were performed. The results from the system validation measurements in the particular bands are summarized in Table 18.

|  |  | f | SAR (W/kg) |  | SAR target (1W) |  | **Difference** | |
|---|---|---|---|---|---|---|---|---|
| D900 | 20 | 900 | 1.06 | 0.68 | 10.8 | 6.9 | **-1.9%** | **-1.4%** |
| D1800 | 20 | 1800 | 4.01 | 2.13 | 38.1 | 19.9 | **5.2%** | **7.0%** |
| D1950 | 20 | 1950 | 4.38 | 2.26 | 40.8 | 21.0 | **7.4%** | **7.6%** |
| D2450 | 17 | 2450 | 2.76 | 1.27 | 54.8 | 25.0 | **0.5%** | **1.4%** |
| D5GHz | 20 | 5200 | 8.65 | 2.49 | 84.0 | 23.6 | **3.0%** | **5.5%** |
| D5GHz | 20 | 5800 | 9.15 | 2.62 | 86.4 | 24.1 | **5.9%** | **8.7%** |

Table 18: Results of the system performance measurements.

## 8.2 PC cards

### 8.2.1 Dosimetric Evaluation

The PC cards have been assessed dosimetrically in the orientations shown in Figure 9.



(a) 3COM XJACK (IEEE802.11a/b/g)



(b) Globetrotter Fusion (EGPRS, UMTS, IEEE802.11b/g)

(c) Belkin F5D8010 (IEEE802.11b/g)
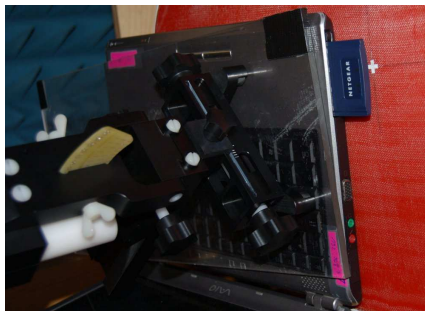


(d) Netgear WAG511GE (IEEE802.11a/b/g)
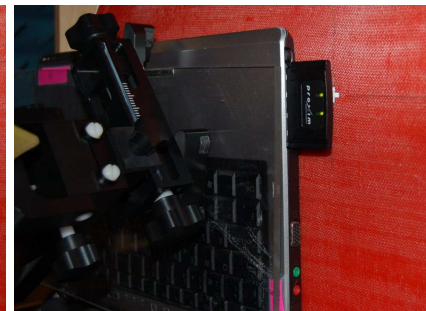
(e) Proxim ORiNOCO (IEEE802.11a/b/g)

Figure 9: PC cards positioned on the elliptical phantom.

**UMTS**  The results of the dosimetric evaluation with a UMTS connection at maximum output power level are summarized in Table 19. Figure 10 displays the SAR distribution inside the tissue simulating liquid for the tested frequencies.

| | | SAR (W/kg) | | |
|---|---|---|---|---|
| **DUT** | **f** | **1g** | **10g** | **Configuration** |
| **Globetrotter Fusion** | **1922.4** | **0.196** | **0.123** | 384kBps uplink |
| Globetrotter Fusion | 1950.0 | 0.195 | 0.121 | 384kBps uplink |
| Globetrotter Fusion | 1977.6 | 0.143 | 0.089 | 384kBps uplink |

Table 19: Globetrotter Fusion peak spatial average SAR in the UMTS band (maximum is bold).



(a) SAR distribution of Globetrotter Fusion (1922.4 MHz)

(b) SAR distribution of Globetrotter Fusion (1950.0 MHz)

(c) SAR distribution of Globetrotter Fusion (1977.6 MHz)
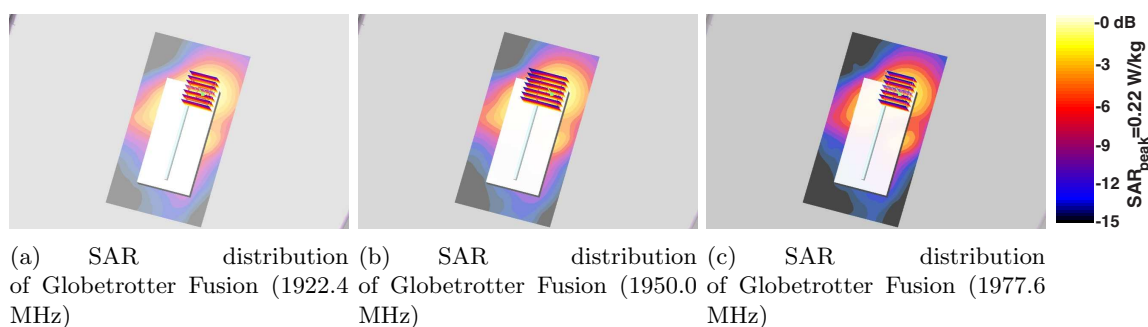
Figure 10: SAR distributions of the Globetrotter Fusion device in the UMTS band.

**EGPRS**  The spatial average peak SAR results for the 900 MHz and 1800 MHz bands of the Globetrotter Fusion are summarized in Tables 20. The corresponding SAR distributions are displayed in Figures 11.

| | | SAR (W/kg) | | |
|---|---|---|---|---|
| **DUT** | **f** | **1g** | **10g** | **Configuration** |
| Globetrotter Fusion | 890.2 | 0.84 | 0.60 | 2 slot usage |
| Globetrotter Fusion | 902.4 | 0.90 | 0.63 | 2 slot usage |
| **Globetrotter Fusion** | **915.8** | **0.95** | **0.67** | 2 slot usage |
| | | | | |
| **Globetrotter Fusion** | **1710.2** | **0.434** | **0.284** | 2 slot usage |
| Globetrotter Fusion | 1747.4 | 0.338 | 0.218 | 2 slot usage |
| Globetrotter Fusion | 1784.8 | 0.270 | 0.175 | 2 slot usage |

Table 20: Globetrotter Fusion peak spatial average SAR in the EGPRS 900 and 1800 bands (maxima are bold).
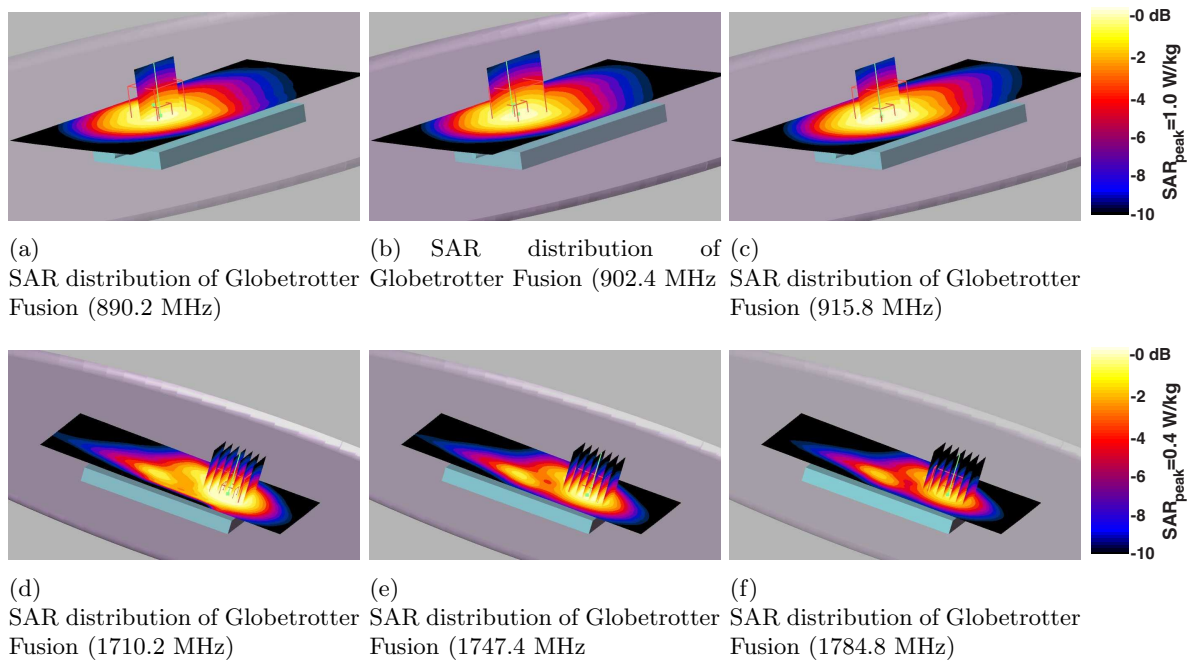
(a)
SAR distribution of Globetrotter Fusion (890.2 MHz)

(b) SAR distribution of Globetrotter Fusion (902.4 MHz

(c) SAR distribution of Globetrotter Fusion (915.8 MHz)

(d)
SAR distribution of Globetrotter Fusion (1710.2 MHz)

(e)
SAR distribution of Globetrotter Fusion (1747.4 MHz

(f)
SAR distribution of Globetrotter Fusion (1784.8 MHz)

Figure 11: SAR distributions of the Globetrotter Fusion device using the EGPRS 900 and 1800 communication system (with 2 slot usage).

**IEEE802.11b/g** The SAR results for the PC cards (Globetrotter Fusion & Belkin F5D8010) tested in IEEE802.11b/g modes as well as the maximum achievable net data rates during the testing are summarized in Tables 21 and 22. The corresponding SAR distributions in the tissue simulating liquid are displayed in Figures 12 and 13.

| DUT | f | SAR (W/kg) 1g | 10g | Configuration |
|-----|---|-----|------|---------------|
| **Globetrotter Fusion** | **2412.0** | **0.220** | **0.127** | IEEE802.11b, data rate during test: 6Mbps |
| Globetrotter Fusion | 2442.0 | 0.216 | 0.118 | IEEE802.11b, data rate during test: 6Mbps |
| Globetrotter Fusion | 2472.0 | 0.178 | 0.098 | IEEE802.11b, data rate during test: 6Mbps |
| | | | | |
| **Globetrotter Fusion** | **2412.0** | **0.110** | **0.064** | IEEE802.11g, data rate during test: 26Mbps |
| Globetrotter Fusion | 2442.0 | 0.055 | 0.033 | IEEE802.11g, data rate during test: 26Mbps |
| Globetrotter Fusion | 2472.0 | 0.057 | 0.034 | IEEE802.11g, data rate during test: 26Mbps |

Table 21: Globetrotter Fusion peak spatial average SAR in the 2450 MHz band (maxima are bold).

| DUT | f | SAR (W/kg) 1g | 10g | Configuration |
|-----|---|-----|------|---------------|
| **Belkin F5D8010** | **2412.0** | **0.77** | **0.425** | IEEE802.11b, data rate during test: 6.3Mbps |
| Belkin F5D8010 | 2442.0 | 0.68 | 0.375 | IEEE802.11b, data rate during test: 6.3Mbps |
| Belkin F5D8010 | 2472.0 | 0.354 | 0.197 | IEEE802.11b, data rate during test: 6.3Mbps |
| | | | | |
| **Belkin F5D8010** | **2412.0** | **0.185** | **0.105** | IEEE802.11g, data rate during test: 21.5Mbps |
| Belkin F5D8010 | 2442.0 | 0.092 | 0.059 | IEEE802.11g, data rate during test: 21.5Mbps |
| Belkin F5D8010 | 2472.0 | 0.045 | 0.029 | IEEE802.11g, data rate during test: 21.5Mbps |

Table 22: Belkin F5D8010 peak spatial average SAR in the 2450 MHz band (maxima are bold).
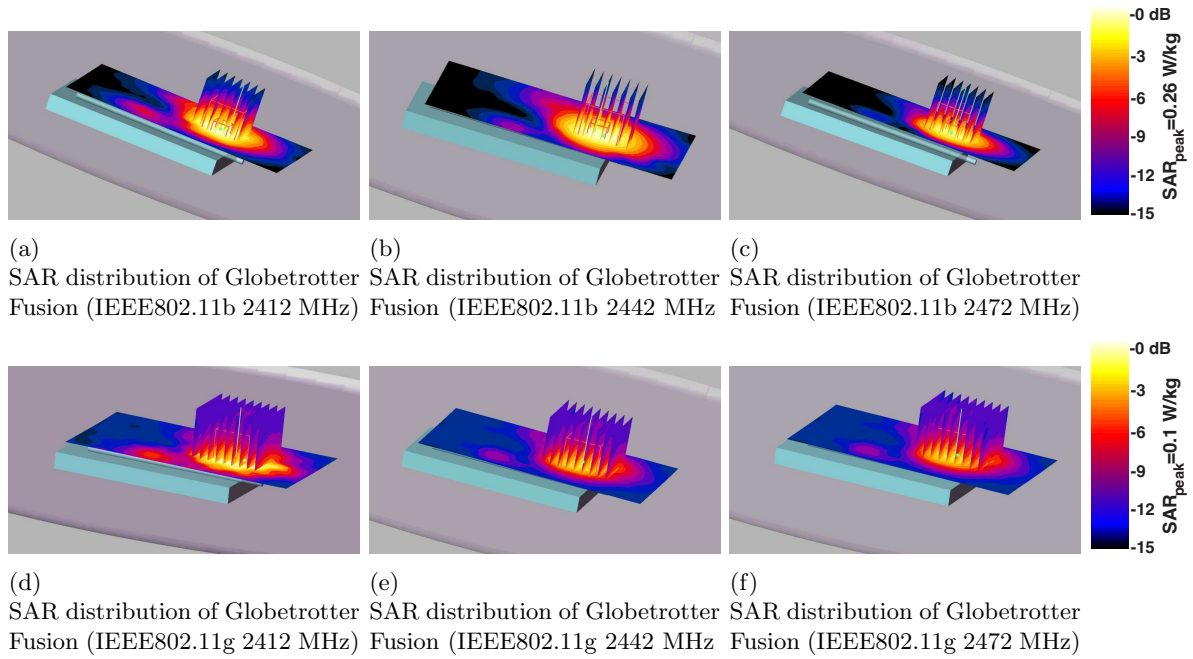
(a)
SAR distribution of Globetrotter Fusion (IEEE802.11b 2412 MHz)

(b)
SAR distribution of Globetrotter Fusion (IEEE802.11b 2442 MHz)

(c)
SAR distribution of Globetrotter Fusion (IEEE802.11b 2472 MHz)

(d)
SAR distribution of Globetrotter Fusion (IEEE802.11g 2412 MHz)

(e)
SAR distribution of Globetrotter Fusion (IEEE802.11g 2442 MHz)

(f)
SAR distribution of Globetrotter Fusion (IEEE802.11g 2472 MHz)

Figure 12: SAR distributions of the Globetrotter Fusion device in the 2450 MHz band.



(a)                    SAR distribution of Belkin F5D8010 (IEEE802.11b 2412 MHz)

(b)                    SAR distribution of Belkin F5D8010 (IEEE802.11b 2442 MHz

(c)                    SAR distribution of Belkin F5D8010 (IEEE802.11b 2472 MHz)

(d)    SAR    distribution of Belkin F5D8010 (IEEE802.11g 2412 MHz)

(e)    SAR    distribution of Belkin F5D8010 (IEEE802.11g 2442 MHz

(f)    SAR    distribution of Belkin F5D8010 (IEEE802.11g 2472 MHz)
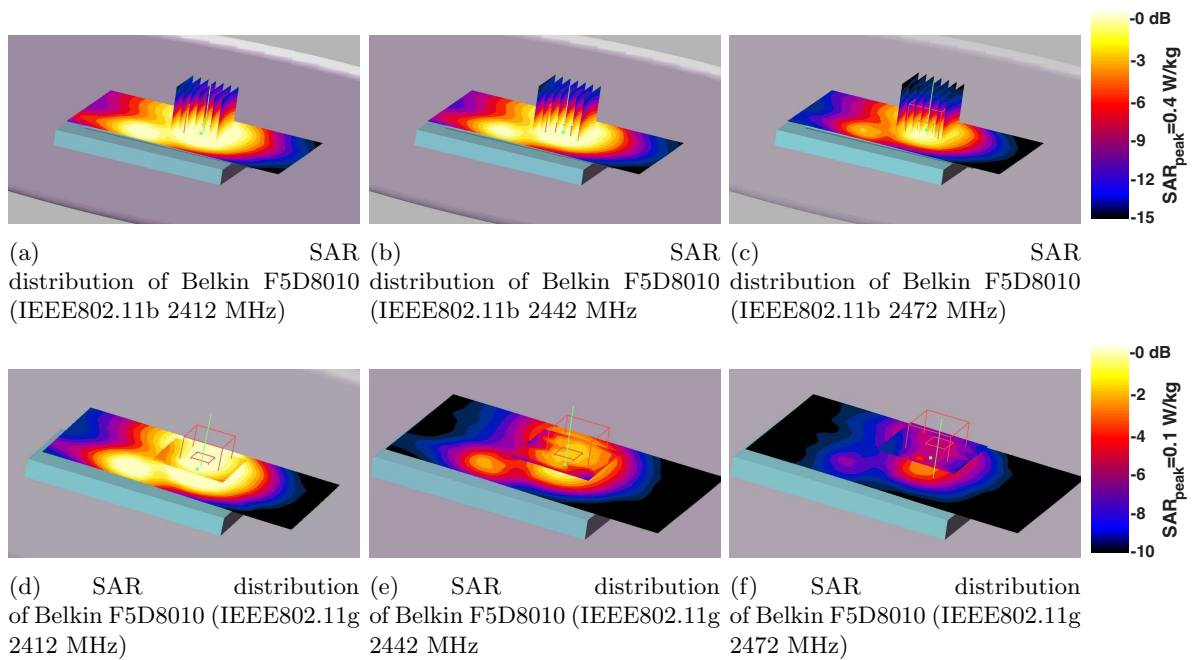
Figure 13: SAR distributions of the Belkin F5D8010 device in the 2450 MHz band.

**IEEE802.11a** The SAR measurement results for the Netgear and Proxim IEEE802.11a WLAN PC card are summarized in Table 23. The corresponding SAR distributions can be found in Figure 14. For the 3com PC card we experienced a strong difference in consecutive area scans. This means that the two-dimensional SAR distributions changed from measurement to measurement (see Figure 15). This behavior can only be explained by usage of spatial antenna diversity in this card. However, this feature is neither documented nor can it be switched off by the card software. Therefore we carried out a total of six consecutive 2-D scan with 3-D scans at the 2-D scans maxima. From the 3-D data we calculated the spatial average SAR (Table 24). As a worst-case assumption, we took the maximum determined spatial average SAR and added the ratio of the minimum and maximum readings, i.e., 10 dB.

| DUT | f | SAR (W/kg) 1g | 10g | Configuration |
|---|---|---|---|---|
| **Netgear WAG511GE** | **5180.0** | **0.087** | **0.050** | IEEE802.11a, data rate during test: 13.3Mbps |
| Netgear WAG511GE | 5240.0 | 0.077 | 0.051 | IEEE802.11a, data rate during test: 13.3Mbps |
| Netgear WAG511GE | 5320.0 | 0.083 | 0.064 | IEEE802.11a, data rate during test: 13.3Mbps |
| | | | | |
| **Proxim ORiNOCO 11** | **5180.0** | **0.106** | **0.069** | IEEE802.11a, data rate during test: 13.3Mbps |
| Proxim ORiNOCO 11 | 5240.0 | 0.102 | 0.063 | IEEE802.11a, data rate during test: 13.3Mbps |
| Proxim ORiNOCO 11 | 5320.0 | 0.080 | 0.062 | IEEE802.11a, data rate during test: 13.3Mbps |

Table 23: Netgear WAG511GE (b/g/a) and Proxim ORiNOCO 11b/g/a peak spatial average SAR in the 2450 MHz band (maxima are bold).



(a) SAR distribution of Netgear WAG511GE (IEEE802.11a 5180 MHz)

(b) SAR distribution of Netgear WAG511GE (IEEE802.11a 5240 MHz

(c) SAR distribution of Netgear WAG511GE (IEEE802.11a 5320 MHz)

(d) SAR distribution of Proxim ORiNOCO (IEEE802.11a 5180 MHz)

(e) SAR distribution of Proxim ORiNOCO (IEEE802.11a 5240 MHz

(f) SAR distribution of Proxim ORiNOCO (IEEE802.11a 5320 MHz)
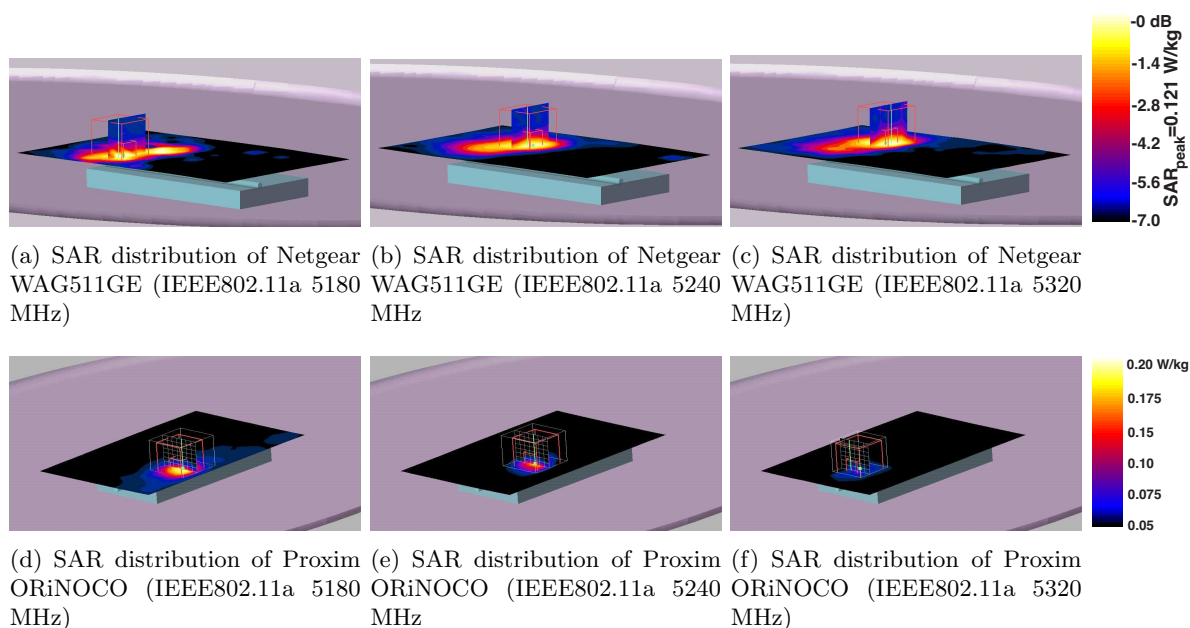
Figure 14: SAR distributions of the Netgear WAG511GE and Proxim ORiNOCO devices in the 5-6 GHz band.

(a) SAR distribution of 2-d scan of 3COM XJACK (IEEE802.11a 5180 MHz)

(b) SAR distribution of 2-d scan 3COM XJACK (IEEE802.11a 5240 MHz
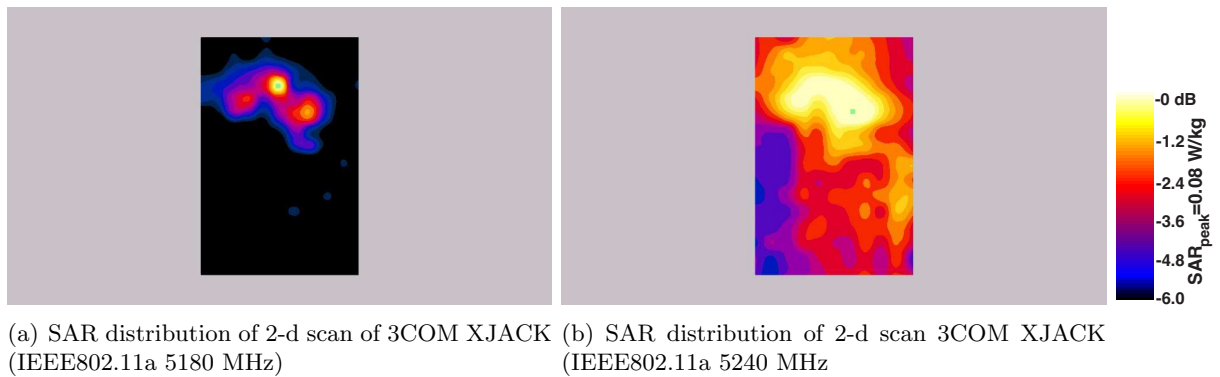
Figure 15: Two dimensional SAR distributions from 3COM PC card with XJACK antenna of two consecutive scans.

| DUT | f | SAR (W/kg) | | Configuration |
| | | 1g | 10g | |
|---|---|---|---|---|
| 3Com XJACK | 5180.0 | 0.049 | 0.047 | IEEE802.11a, data rate during test: 13.3Mbps |
| 3Com XJACK | 5180.0 | 0.011 | 0.007 | IEEE802.11a, data rate during test: 13.3Mbps |
| 3Com XJACK | 5180.0 | 0.012 | 0.007 | IEEE802.11a, data rate during test: 13.3Mbps |
| **3Com XJACK** | **5180.0** | **0.072** | **0.063** | IEEE802.11a, data rate during test: 13.3Mbps |
| 3Com XJACK | 5180.0 | 0.052 | 0.048 | IEEE802.11a, data rate during test: 13.3Mbps |
| 3Com XJACK | 5180.0 | 0.010 | 0.006 | IEEE802.11a, data rate during test: 13.3Mbps |

Table 24: 3COM PC card peak spatial average SAR in the 5 GHz band (maximum is bold). Due to unstable measurement the results show a worst-case variation of 10 dB. If this variation is applied to the maximum measured spatial peak SAR, this corresponds to a $SAR_{1g}$ of 0.72 W/kg and a $SAR_{10g}$ of 0.63 W/kg.

### 8.2.2   Incident E&H-Fields

The incident E-fields have been assessed for the Globetrotter Fusion (EGPRS, UMTS), the Belkin (IEEE802.11b/g) and the 3COM XJACK (IEEE802.11a) PC cards. The maximum E-field at a constant distance with the DUT rotating along three mutually perpendicular rotation axes has been previously determined; the E-fields were then mapped over distance in this direction.

**EGPRS**   The measurements were taken in the 900 and 1800 MHz EGPRS bands. In order to preserve battery power over the measurement time, the measurements were taken at 29 and 26 dBm peak output power and extrapolated to the field strength at 33 dBm and 30 dBm. The resulting E-field distributions are shown in Figures 16, 17. In the near field of the device the incident H-fields were determined as well. The results are displayed in Figures 18, 19.
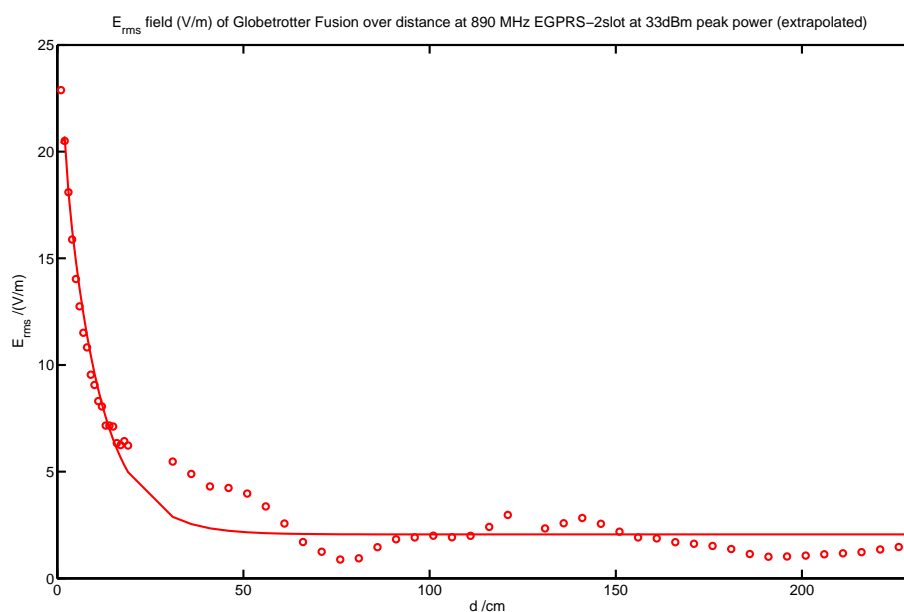


Figure 16: Globetrotter Fusion E-field over distance (EGPRS900).
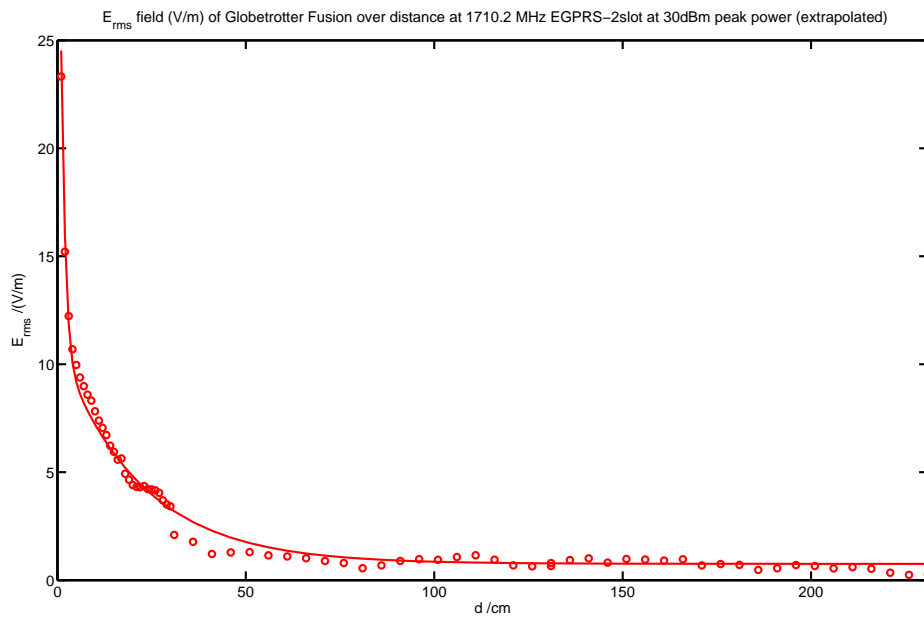
Figure 17: Globetrotter Fusion E-field over distance (EGPRS1800).
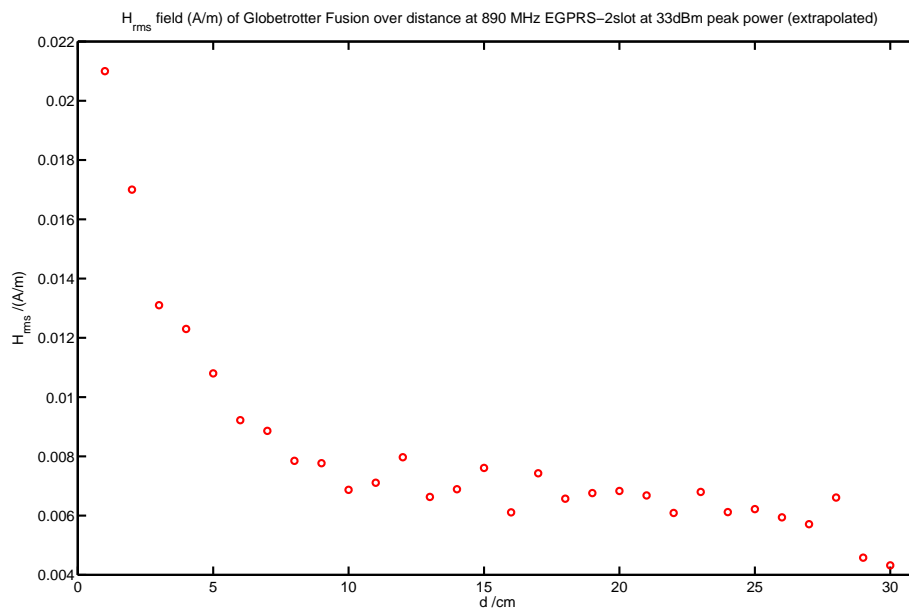


Figure 18: Globetrotter Fusion H-Field over distance (EGPRS900).
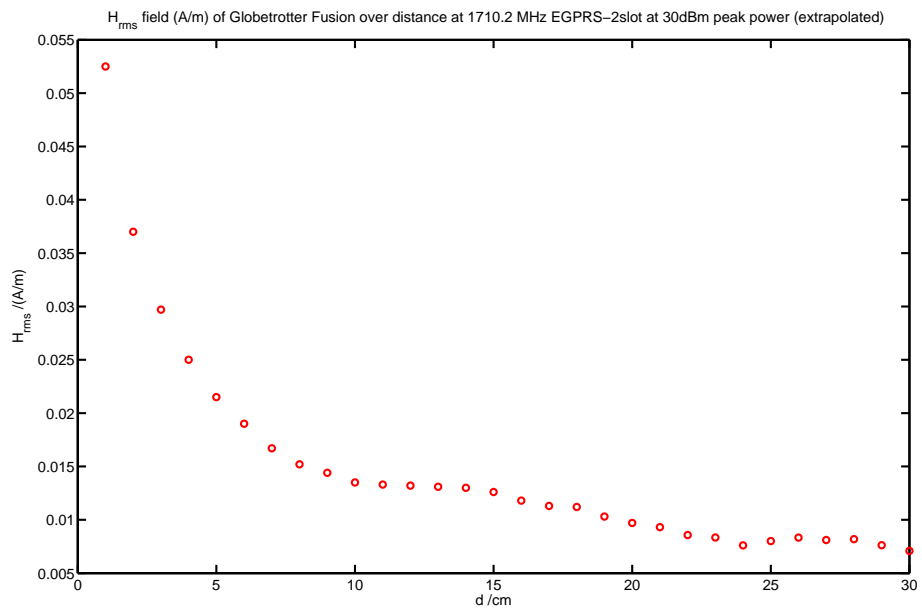
Figure 19: Globetrotter Fusion H-Field over distance (EGPRS1800).

**UMTS** The measurements were taken at maximum output power using the UMTS communication link. The resulting E-field distributions are shown in Figure 20. In the near field of the device the incident H-fields were determined as well. The results are displayed in Figure 21.
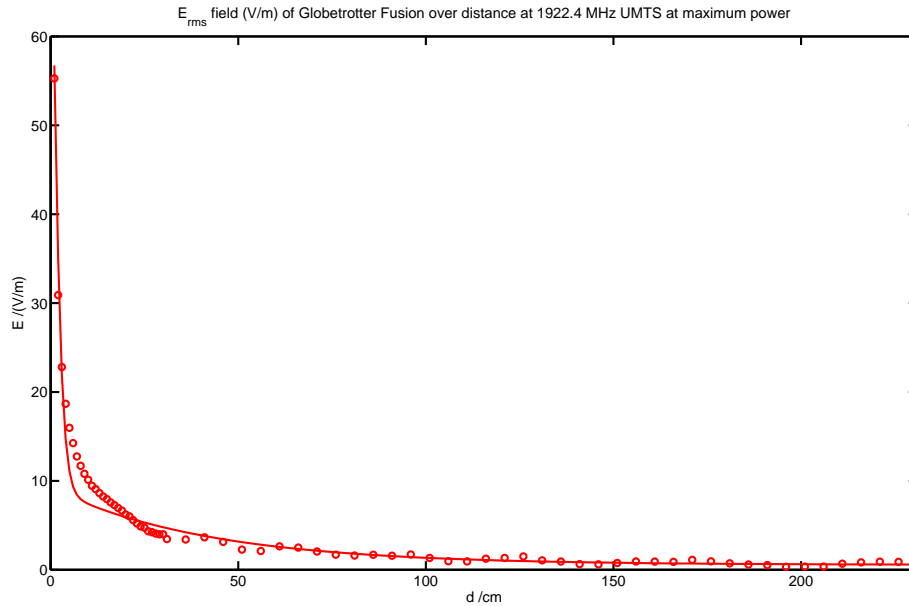


Figure 20: Globetrotter Fusion E-field over distance (UMTS).
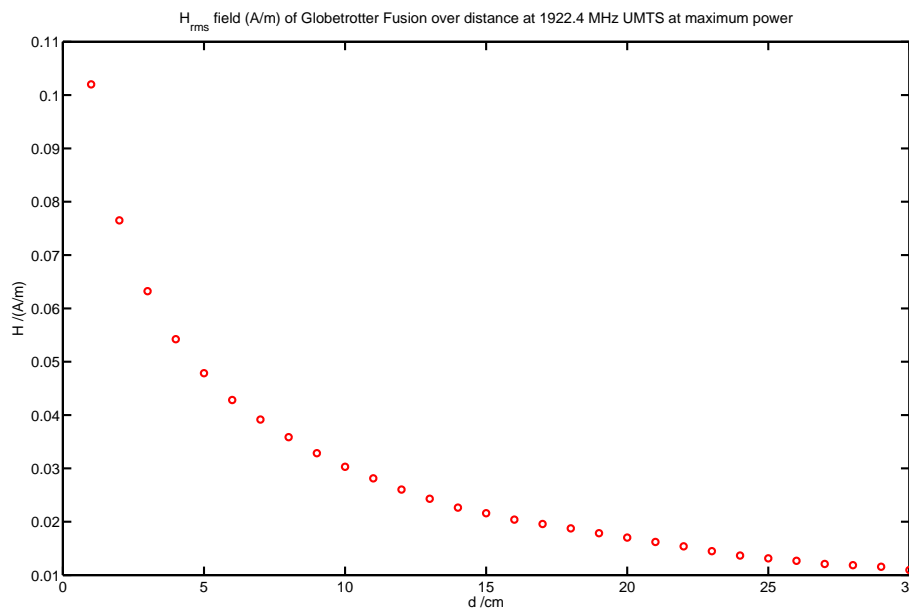


Figure 21: Globetrotter Fusion H-field over distance (UMTS).

**IEEE802.11b/g** The measurements were taken at maximum output power in IEEE802.11b mode for the Belkin PC card and extrapolated for IEEE802.11g mode using the rms power ratio between both modes. The resulting E-field distributions are shown in Figures 22 and 23. In the near field of the device the incident H-fields were determined as well. The results are displayed in Figures 24 and 25.
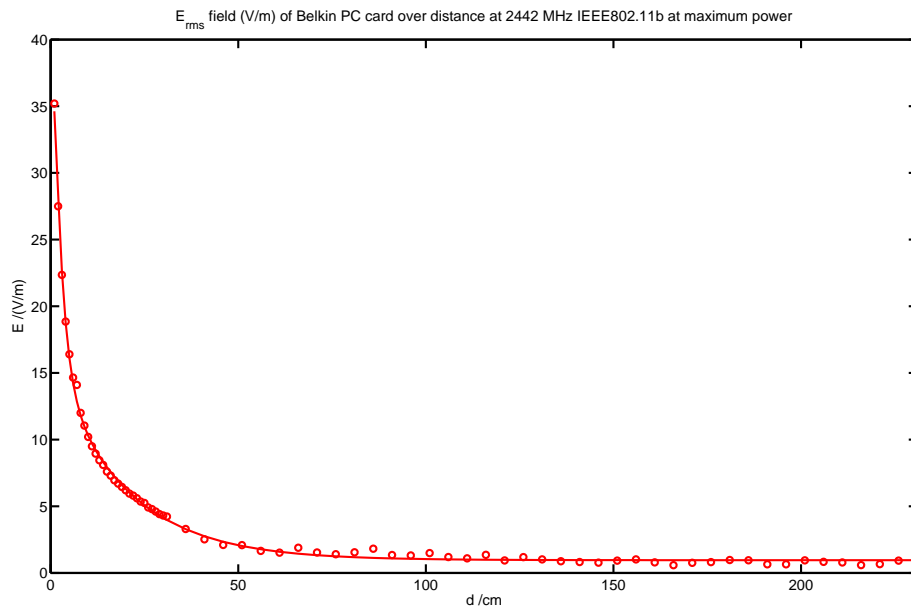


Figure 22: Belkin PC card E-field over distance in the IEEE802.11b communication system.
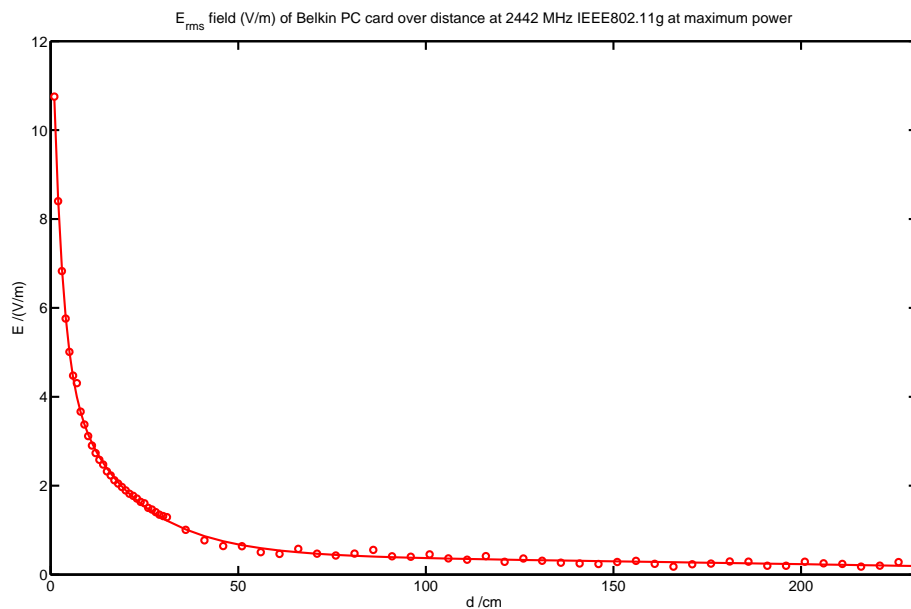


Figure 23: Belkin PC card E-field over distance in the IEEE802.11g communication system (extrapolated).
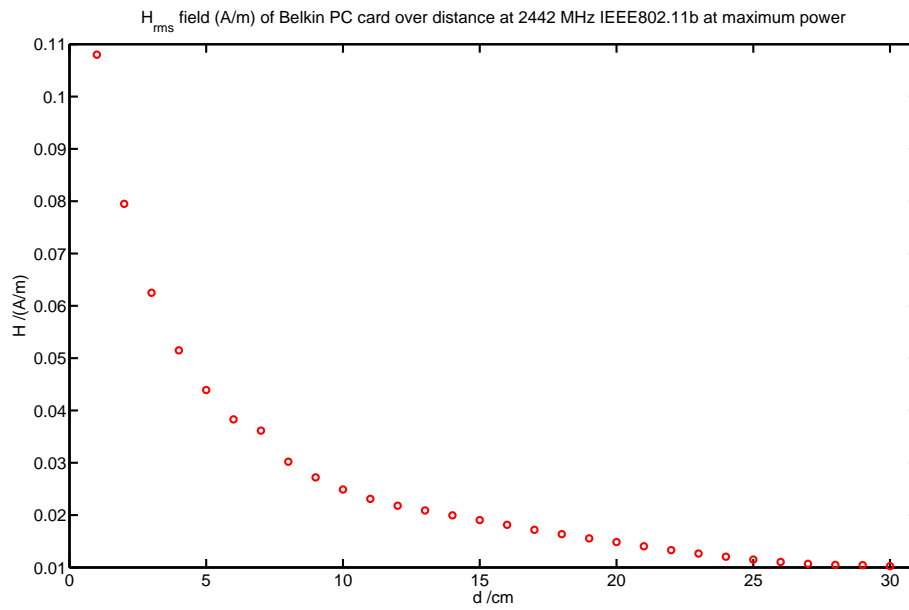
Figure 24: Belkin PC card H-field over distance in the IEEE802.11b communication system.
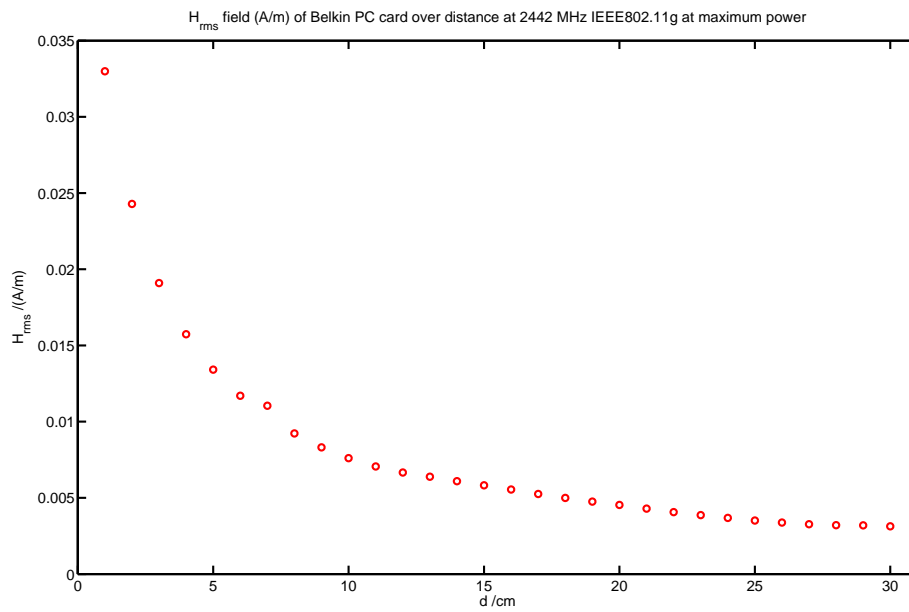


Figure 25: Belkin PC card H-field over distance in the IEEE802.11g communication system (extrapolated).

**IEEE802.11a** The measurements were taken at maximum output power in IEEE802.11a mode for the 3COM PC card. The resulting E-field distributions are shown in Figure 26.
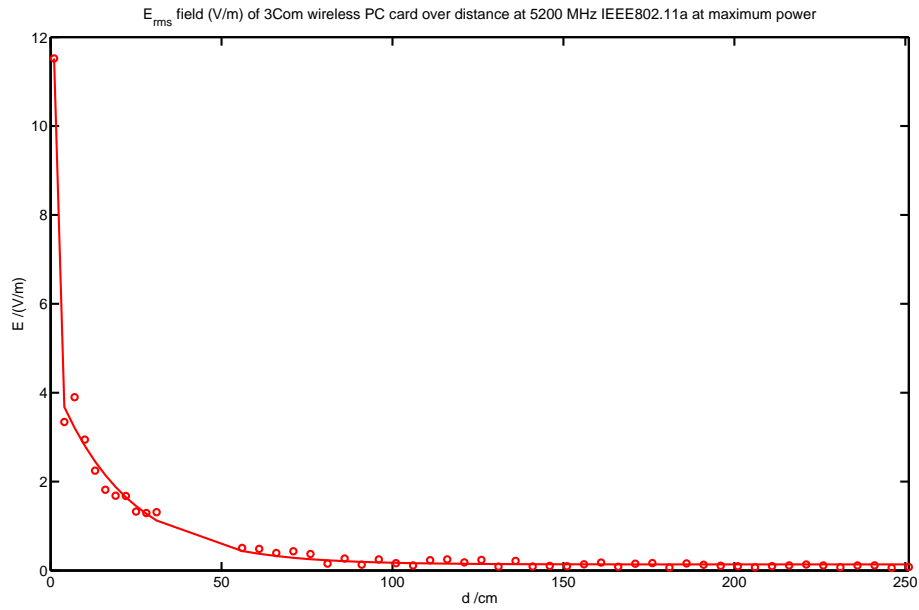


Figure 26: 3 Com XJACK E-field over distance in the IEEE802.11a communication system.

## 8.3 Access Points

### 8.3.1 Dosimetric Evaluation

The access points have been assessed dosimetrically in the orientations shown in Figure 30. The Cisco Aironet 1200 access points have been tested in two orientations (Figures 30(a), 30(b)) attached to the elliptical phantom to determine the worst-case absorption orientation. The frequency dependence of the absorption has then been tested in this worst-case position. The Aironet 1200 access points are physically identical but were configured as root bridge and non root bridge by Swisscom Innovations, respectively. For the Enterasys (Figure 27), Netgear (Figure 28) and LinkSys (Figure 29) access points we employed the fast dosimetric scanner (iSAR, SPEAG) to determine the worst-case orientation. Additionally, we used iSAR to determine the worst-case absorption with respect to antenna diversity and single antennas switched on. The corresponding worst-case positions were then used on the elliptical phantom (Figures 30(c), 30(d)). The peak spatial average SAR results are summarized in Tables 25, 26, 27, and 28. The corresponding SAR distributions in the tissue simulating liquid are shown in Figures 31, 32, 33 , 34, and 35.



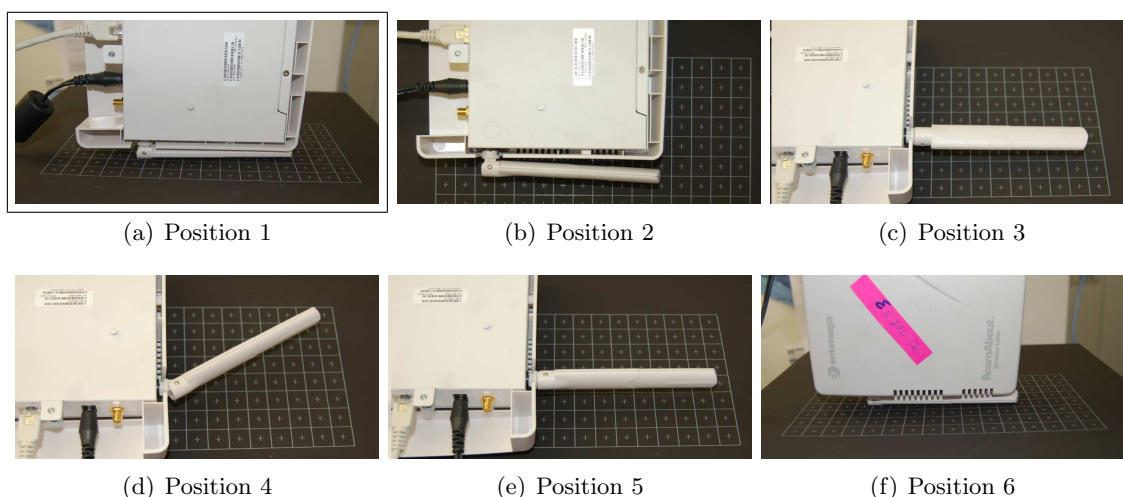| (a) Position 1 | (b) Position 2 | (c) Position 3 |
| (d) Position 4 | (e) Position 5 | (f) Position 6 |

Figure 27: Enterasys Roamabout RBT-4102 positions on the iSAR scanner. Worst-case is indicated with a frame (identical orientation for IEEE802.11a/b).



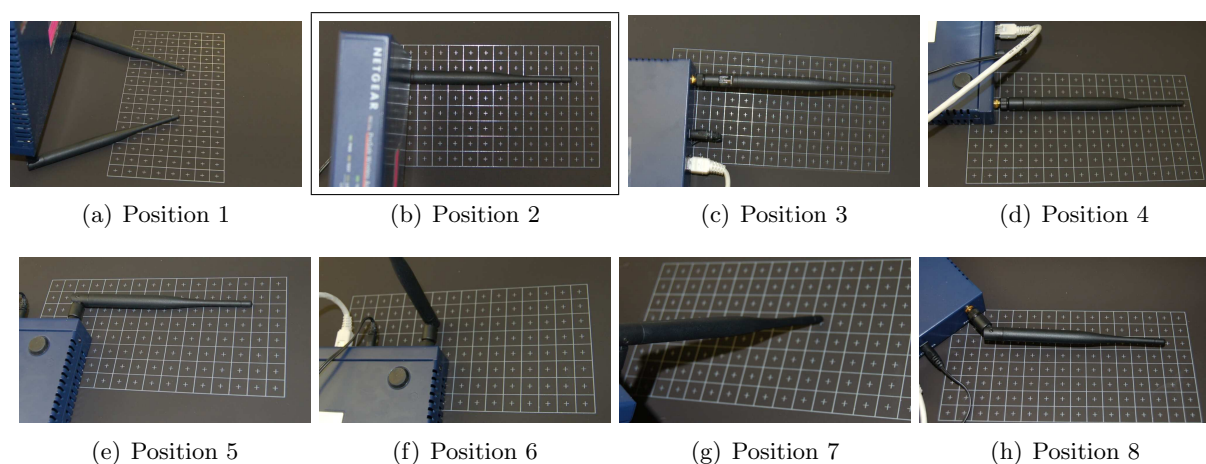| (a) Position 1 | (b) Position 2 | (c) Position 3 | (d) Position 4 |
| (e) Position 5 | (f) Position 6 | (g) Position 7 | (h) Position 8 |

Figure 28: Netgear ProSafe WG302 802.11g positions on the iSAR scanner. Worst-case is indicated with a frame (identical orientation for IEEE802.11a/b).

(a) Position 1     (b) Position 2     (c) Position 3 (worst-case in 5.6 GHz band)     (d) Position 4 (worst-case in 5.25 GHz band)
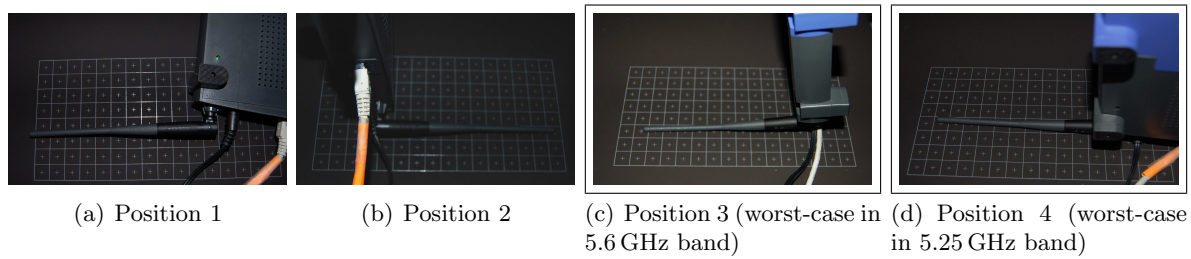
Figure 29: Linksys 55AG (IEEE802.11a mode) positions on the iSAR scanner. Worst-cases in upper and lower 5 GHz band are indicated with frames.



(a) Aironet 1200 Root Bridge and Non Root Bridge in flat orientation (IEEE802.11a)

(b) Aironet 1200 Root Bridge and Non Root Bridge in perpendicular orientation (worst-case) (IEEE802.11a)

(c) Enterasys Roamabout RBT-4102 worst-case orientation (IEEE802.11a/b/g)

(d) Netgear ProSafe WG302 802.11g worst case orientation (IEEE802.11b/g)

Figure 30: Access points positioned on the elliptical phantom.

| DUT | f | SAR (W/kg) | | Configuration |
|---|---|---|---|---|
| | | 1g | 10g | |
| **ENTERASYS RBT-4102** | **2412.0** | **1.47** | **0.73** | IEEE802.11b, data rate during test: 6Mbps |
| ENTERASYS RBT-4102 | 2442.0 | 1.27 | 0.64 | IEEE802.11b, data rate during test: 6Mbps |
| ENTERASYS RBT-4102 | 2472.0 | 0.93 | 0.409 | IEEE802.11b, data rate during test: 6Mbps |
| | | | | |
| **ENTERASYS RBT-4102** | **2412.0** | **0.58** | **0.274** | IEEE802.11g, data rate during test: 26Mbps |
| ENTERASYS RBT-4102 | 2442.0 | 0.467 | 0.229 | IEEE802.11g, data rate during test: 26Mbps |
| ENTERASYS RBT-4102 | 2472.0 | 0.349 | 0.164 | IEEE802.11g, data rate during test: 26Mbps |
| | | | | |
| ENTERASYS RBT-4102 | 5180 | 0.467 | 0.148 | IEEE802.11a, data rate during test: 6Mbps |
| ENTERASYS RBT-4102 | 5240 | 0.473 | 0.152 | IEEE802.11a, data rate during test: 6Mbps |
| **ENTERASYS RBT-4102** | **5320** | **0.55** | **0.180** | IEEE802.11a, data rate during test: 6Mbps |

Table 25: ENTERASYS RBT-4102 peak spatial average SAR in the 2450 MHz and 5 GHz bands (maxima are bold). 6 Mbps corresponds to the maximum transmission (TX) rate of the ENTERASYS device in IEEE802.11a mode (at higher rates the connection was frequently interrupted).

| DUT | f | SAR (W/kg) | | Configuration |
|---|---|---|---|---|
| | | 1g | 10g | |
| Aironet 1200 root bridge | 5500 | 0.054 | 0.029 | flat, IEEE802.11a, data rate during test: 7-8Mbps |
| Aironet 1200 root bridge | 5500 | 0.107 | 0.032 | perp., IEEE802.11a, data rate during test: 7-8Mbps |
| Aironet 1200 root bridge | 5600 | 0.166 | 0.045 | perp., IEEE802.11a, data rate during test: 7-8Mbps |
| **Aironet 1200 root bridge** | **5700** | **0.419** | **0.100** | perp., IEEE802.11a, data rate during test: 7-8Mbps |
| | | | | |
| Aironet 1200 non root bridge | 5500 | 0.446 | 0.107 | perp., IEEE802.11a, data rate during test: 27-29Mbps |
| Aironet 1200 non root bridge | 5600 | 0.56 | 0.133 | perp., IEEE802.11a, data rate during test: 27-29Mbps |
| **Aironet 1200 non root bridge** | **5700** | **1.59** | **0.359** | perp., IEEE802.11a, data rate during test: 27-29Mbps |

Table 26: Cisco Aironet 1200 root bridge and non root bridge peak spatial average SAR in the 5 GHz band (maxima are bold).

| DUT | f | SAR (W/kg) | | Configuration |
|---|---|---|---|---|
| | | 1g | 10g | |
| **Netgear ProSafe WG302** | **2412.0** | **1.00** | **0.442** | IEEE802.11b, data rate during test: 6Mbps |
| Netgear ProSafe WG302 | 2442.0 | 0.82 | 0.360 | IEEE802.11b, data rate during test: 6Mbps |
| Netgear ProSafe WG302 | 2472.0 | 0.68 | 0.297 | IEEE802.11b, data rate during test: 6Mbps |
| | | | | |
| **Netgear ProSafe WG302** | **2412.0** | **0.55** | **0.245** | IEEE802.11g, data rate during test: 26Mbps |
| Netgear ProSafe WG302 | 2442.0 | 0.467 | 0.213 | IEEE802.11g, data rate during test: 26Mbps |
| Netgear ProSafe WG302 | 2472.0 | 0.402 | 0.157 | IEEE802.11g, data rate during test: 26Mbps |

Table 27: Netgear ProSafe WG302 802.11g peak spatial average SAR in the 2.45 GHz band (maxima are bold).

| | | SAR (W/kg) | | |
|---|---|---|---|---|
| **DUT** | **f** | **1g** | **10g** | **Configuration** |
| Linksys WAG55 AG | 5180 | 0.72 | 0.222 | IEEE802.11a, data rate during test: 29-30 Mbps |
| **Linksys WAG55 AG** | **5240** | **1.59** | **0.391** | IEEE802.11a, data rate during test: 29-30 Mbps |
| Linksys WAG55 AG | 5320 | 1.14 | 0.347 | IEEE802.11a, data rate during test: 29-30 Mbps |
| | | | | |
| **Linksys WAG55 AG** | **5500** | **1.86** | **0.54** | IEEE802.11a, data rate during test: 29-30 Mbps |
| Linksys WAG55 AG | 5600 | 1.15 | 0.244 | IEEE802.11a, data rate during test: 29-30 Mbps |
| Linksys WAG55 AG | 5700 | 1.06 | 0.313 | IEEE802.11a, data rate during test: 29-30 Mbps |

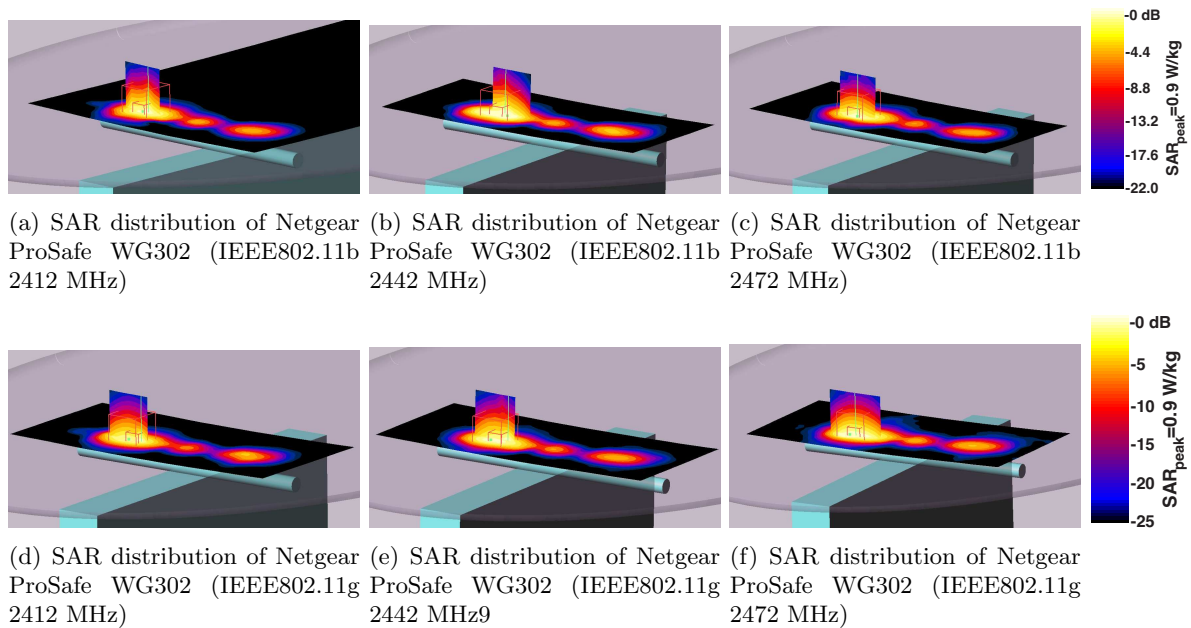Table 28: LinkSys WAG55 AG peak spatial average SAR in the 5 GHz band (maxima are bold).



(a) SAR distribution of Netgear ProSafe WG302 (IEEE802.11b 2412 MHz)

(b) SAR distribution of Netgear ProSafe WG302 (IEEE802.11b 2442 MHz)

(c) SAR distribution of Netgear ProSafe WG302 (IEEE802.11b 2472 MHz)

(d) SAR distribution of Netgear ProSafe WG302 (IEEE802.11g 2412 MHz)

(e) SAR distribution of Netgear ProSafe WG302 (IEEE802.11g 2442 MHz9

(f) SAR distribution of Netgear ProSafe WG302 (IEEE802.11g 2472 MHz)

Figure 31: SAR distributions of the Netgear ProSafe WG302 device in the 2450 MHz band.



(a) SAR distribution of ENTERASYS RBT-4102 (IEEE802.11b 2412 MHz)

(b) SAR distribution of ENTERASYS RBT-4102 (IEEE802.11b 2442 MHz)

(c) SAR distribution of ENTERASYS RBT-4102 (IEEE802.11b 2472 MHz)

(d) SAR distribution of ENTERASYS RBT-4102 (IEEE802.11g 2412 MHz)

(e) SAR distribution of ENTERASYS RBT-4102 (IEEE802.11g 2442 MHz

(f) SAR distribution of ENTERASYS RBT-4102 (IEEE802.11g 2472 MHz)
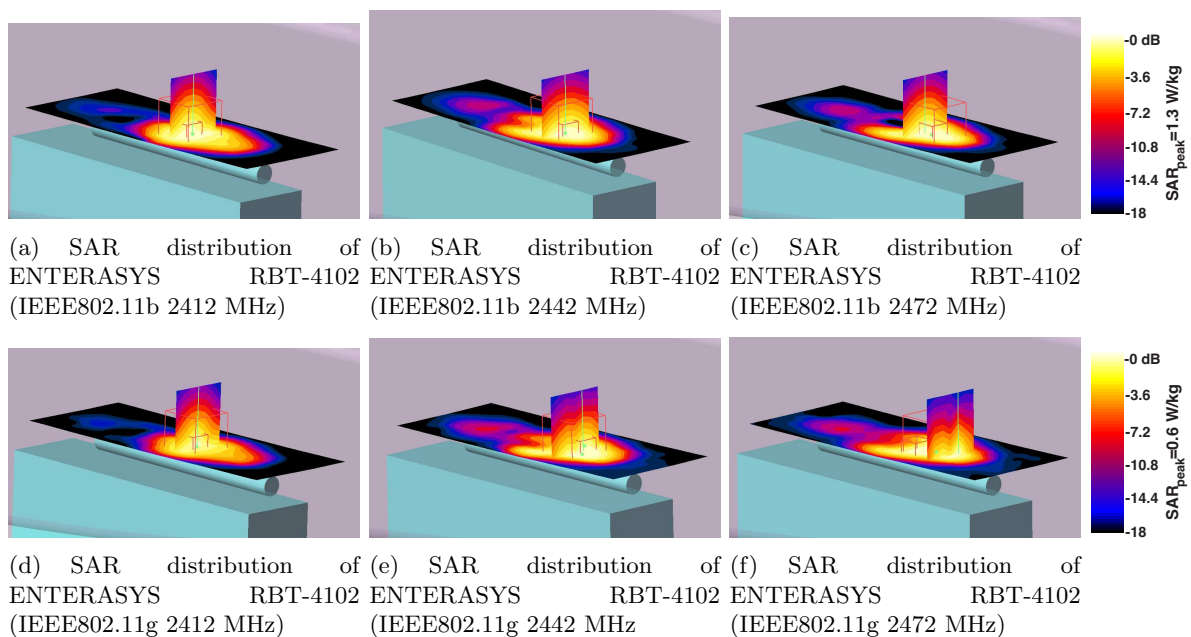
Figure 32: SAR distributions of the ENTERASYS RBT-4102 device in the 2450 MHz band.

(a) SAR distribution of ENTERASYS RBT-4102 (IEEE802.11a 5180 MHz)

(b) SAR distribution of ENTERASYS RBT-4102 (IEEE802.11a 5240 MHz)
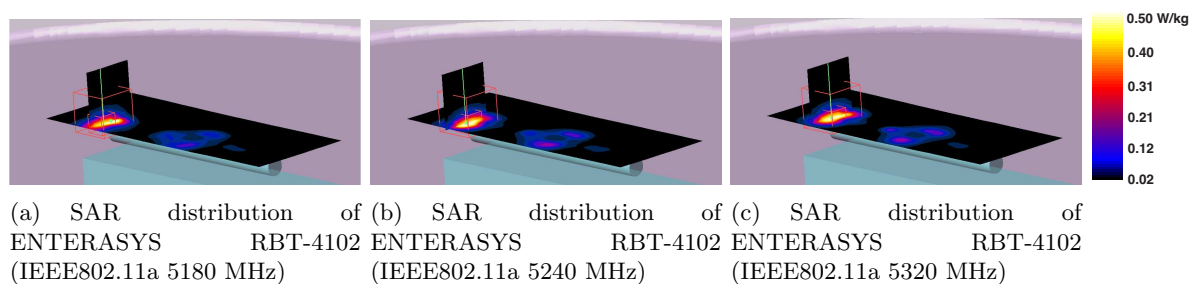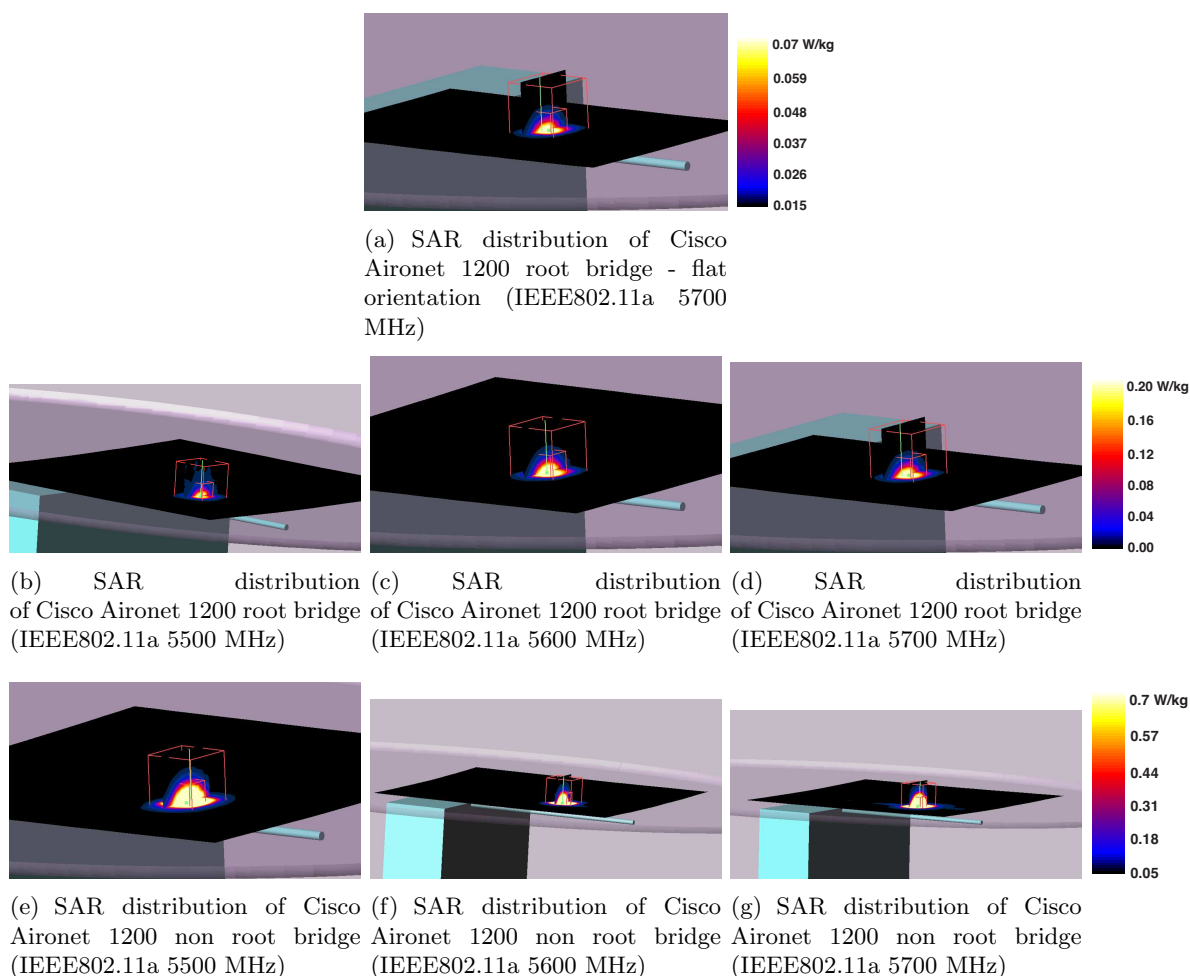
(c) SAR distribution of ENTERASYS RBT-4102 (IEEE802.11a 5320 MHz)

Figure 33: SAR distributions of the ENTERASYS RBT-4102 device in the 5 GHz band.



(a) SAR distribution of Cisco Aironet 1200 root bridge - flat orientation (IEEE802.11a 5700 MHz)



(b) SAR distribution of Cisco Aironet 1200 root bridge (IEEE802.11a 5500 MHz)

(c) SAR distribution of Cisco Aironet 1200 root bridge (IEEE802.11a 5600 MHz)

(d) SAR distribution of Cisco Aironet 1200 root bridge (IEEE802.11a 5700 MHz)



(e) SAR distribution of Cisco Aironet 1200 non root bridge (IEEE802.11a 5500 MHz)

(f) SAR distribution of Cisco Aironet 1200 non root bridge (IEEE802.11a 5600 MHz)

(g) SAR distribution of Cisco Aironet 1200 non root bridge (IEEE802.11a 5700 MHz)

Figure 34: SAR distributions of the Cisco Aironet 1200 non root- and root-bridge in the 5 GHz band.

(a) SAR distribution of LinkSys WAG55 AG (IEEE802.11a 5180 MHz)

(b) SAR distribution of LinkSys WAG55 AG (IEEE802.11a 5240 MHz)

(c) SAR distribution of LinkSys WAG55 AG (IEEE802.11a 5320 MHz)

(d) SAR distribution of LinkSys WAG55 AG (IEEE802.11a 5500 MHz)

(e) SAR distribution of LinkSys WAG55 AG (IEEE802.11a 5600 MHz)

(f) SAR distribution of LinkSys WAG55 AG (IEEE802.11a 5700 MHz)
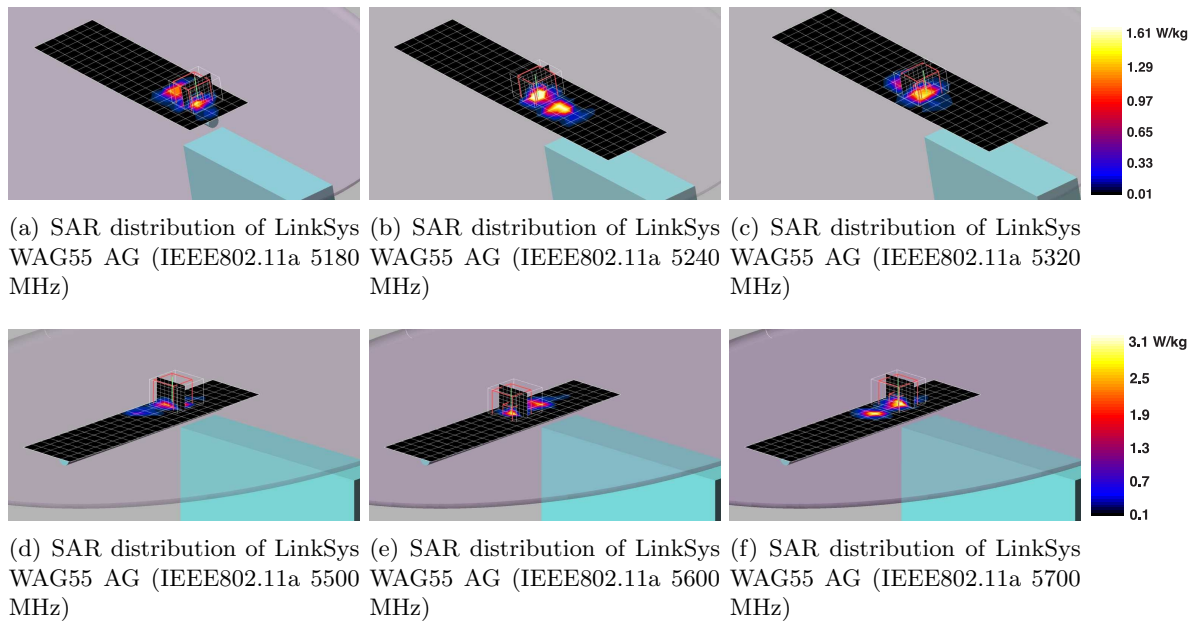
Figure 35: SAR distributions of the LinkSys WAG55 AG in the 5 GHz band.

### 8.3.2 Incident E&H-Fields

The incident E-field has been assessed for the Enterasys Roamabout RBT-4102 access point. The maximum E-field at a constant distance with the DUT rotating along three mutually perpendicular rotation axes has been previously determined, then the E-fields were mapped over distance in the maximum direction.

**IEEE802.11b/g**   The measurements were taken at maximum output power in IEEE802.11b mode and then extrapolated to the IEEE802.11g mode using the determined rms power difference between both modes. The resulting E-field distributions are shown in Figure 36.

In the near field of the device the incident H-fields were determined as well. The results are displayed in Figure 37.



(a) Enterasys Roamabout RBT-4102 access point $E_{rms}$ over distance for IEEE802.11b

(b) Enterasys Roamabout RBT-4102 access point $E_{rms}$ over distance for IEEE802.11g (extrapolated)
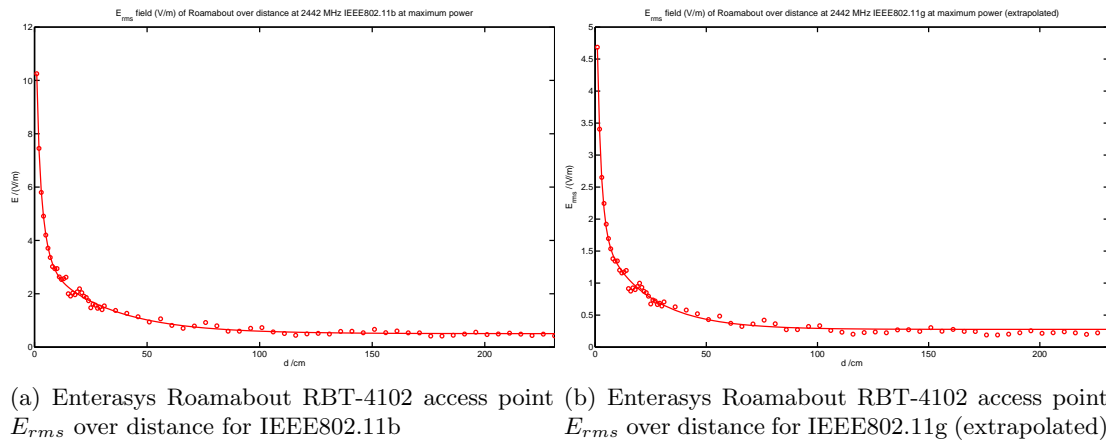
Figure 36: Access point E-field over distance (IEEE802.11b/g).



(a) Enterasys Roamabout RBT-4102 access point $H_{rms}$ over distance for IEEE802.11b

(b) Enterasys Roamabout RBT-4102 access point $H_{rms}$ over distance for IEEE802.11g (extrapolated)
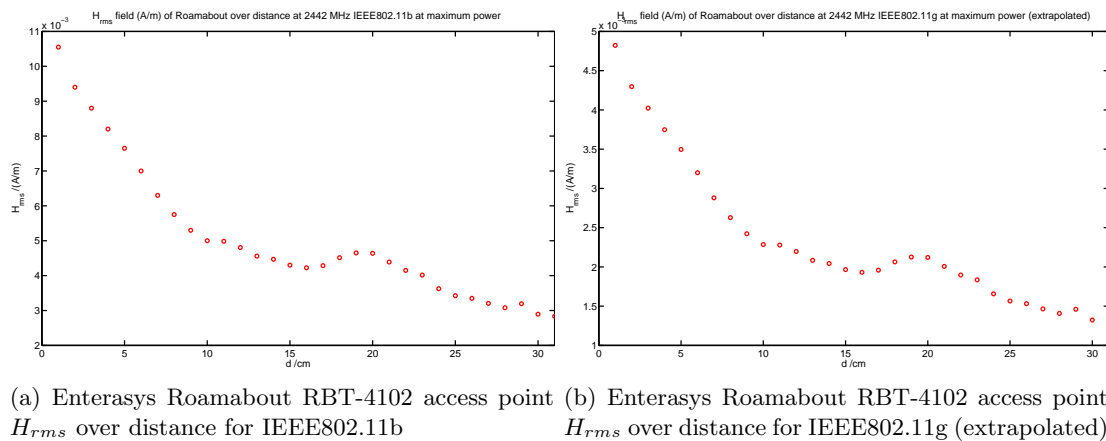
Figure 37: Access point H-Field over distance (IEEE802.11b/g).

**IEEE802.11a**   The resulting E-field distributions for the Enterasys Roamabout RBT-4102 and LinkSys WAG55 AG access points are shown in Figures 38, 39.
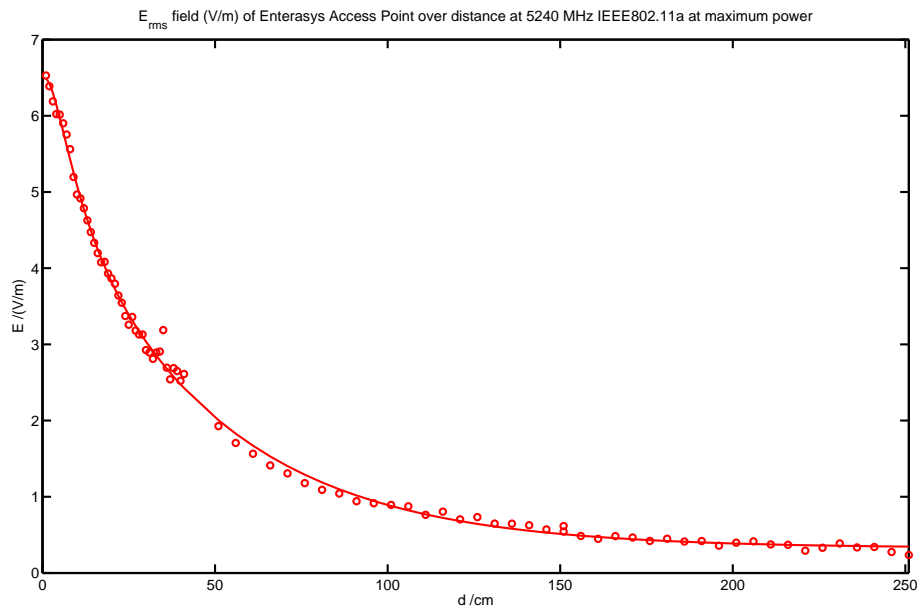
Figure 38: Enterasys access point E-field over distance in IEEE802.11a mode.
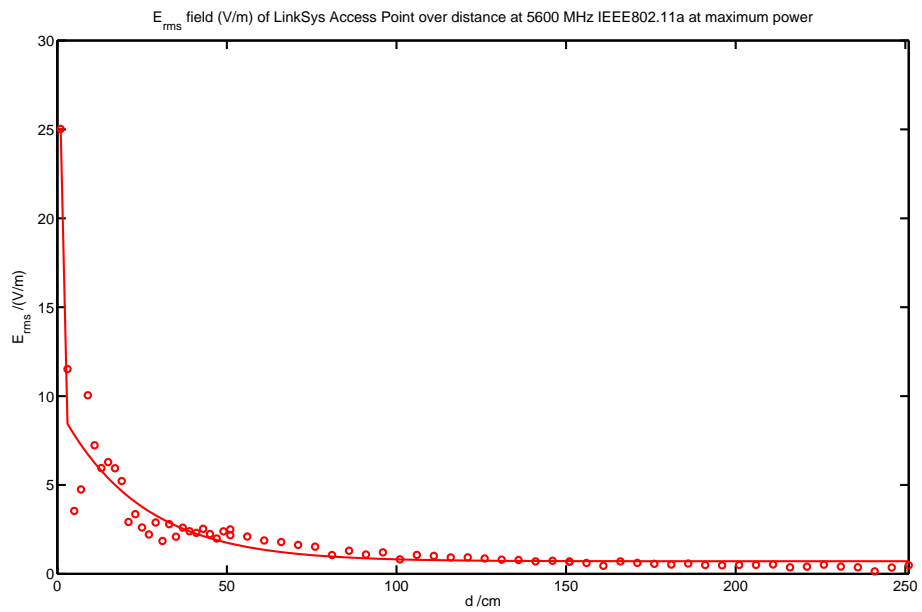


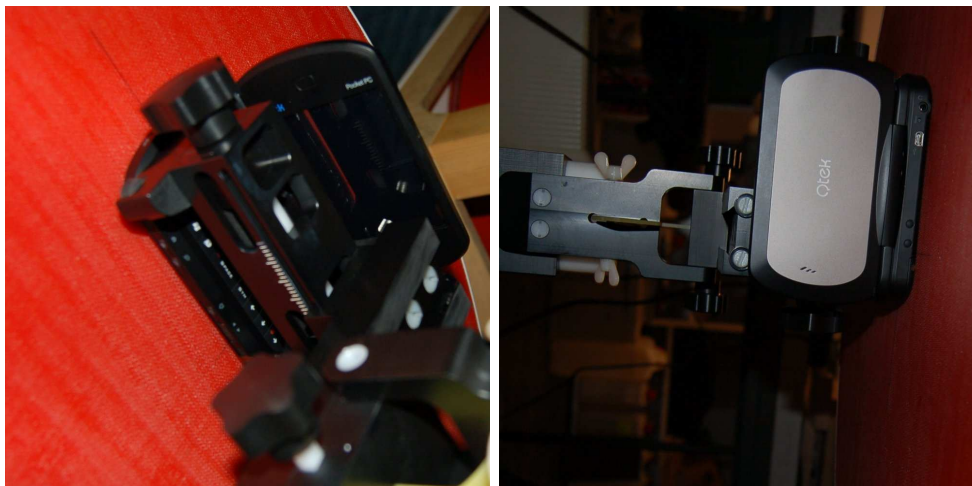Figure 39: Linksys access point E-field over distance in IEEE802.11a mode.

## 8.4  Personal Digital Assistant

### 8.4.1  Dosimetric Evaluation

The QTEK 9000 PDA has been assessed dosimetrically in the orientations shown in Figure 40.



(a) QTEK 9000 in *PDA mode* attached to the phantom



(b) QTEK 9000 in *Laptop mode* (display 180°) attached to the phantom



(c) QTEK 9000 in *Laptop mode* (display 90°) attached to the phantom

Figure 40: Dosimetric assessment orientations of the QTEK 9000 PDA.

**UMTS**   The results of the dosimetric evaluation with a UMTS connection at maximum output power level are summarized in Table 29. Besides the test at the maximum up-link data rate of 384 kBps, the device has also been tested at a 12 kBps up-link data rate. The results confirm the assumption that there is no influence of the applied data rate on the SAR for UMTS. Figure 41 displays the SAR distribution inside the tissue simulating liquid for the tested scenarios.

| DUT | f | SAR (W/kg) | | Configuration |
|---|---|---|---|---|
| | | 1g | 10g | |
| QTEK 9000 | 1922.4 | 3.75 | 1.88 | PDA, 384kBps uplink |
| **QTEK 9000** | **1950.0** | **4.17** | **2.06** | PDA, 384kBps uplink |
| QTEK 9000 | 1977.6 | 3.61 | 1.75 | PDA, 384kBps uplink |
| QTEK 9000 | 1950.0 | 4.16 | 2.05 | PDA, 12kBps uplink |
| QTEK 9000 | 1950.0 | 4.10 | 2.03 | Laptop 90, 384kBps uplink |
| QTEK 9000 | 1950.0 | 4.16 | 2.04 | Laptop 180, 384kBps uplink |

Table 29: QTEK 9000 peak spatial average SAR in the UMTS band (maximum is bold).



(a) SAR distribution of QTEK 9000 (Laptop mode, display 90°, 1950 MHz)

(b) SAR distribution of QTEK 9000 (Laptop mode, display 180°, 1950 MHz)

(c) SAR distribution of QTEK 9000 (PDA mode, 12 kBps, 1950 MHz)

(d) SAR distribution of QTEK 9000 (PDA mode, 384 kBps, 1922.4 MHz)

(e) SAR distribution of QTEK 9000 (PDA mode, 384 kBps, 1950.0 MHz

(f) SAR distribution of QTEK 9000 (PDA mode, 384 kBps, 1977.6 MHz)
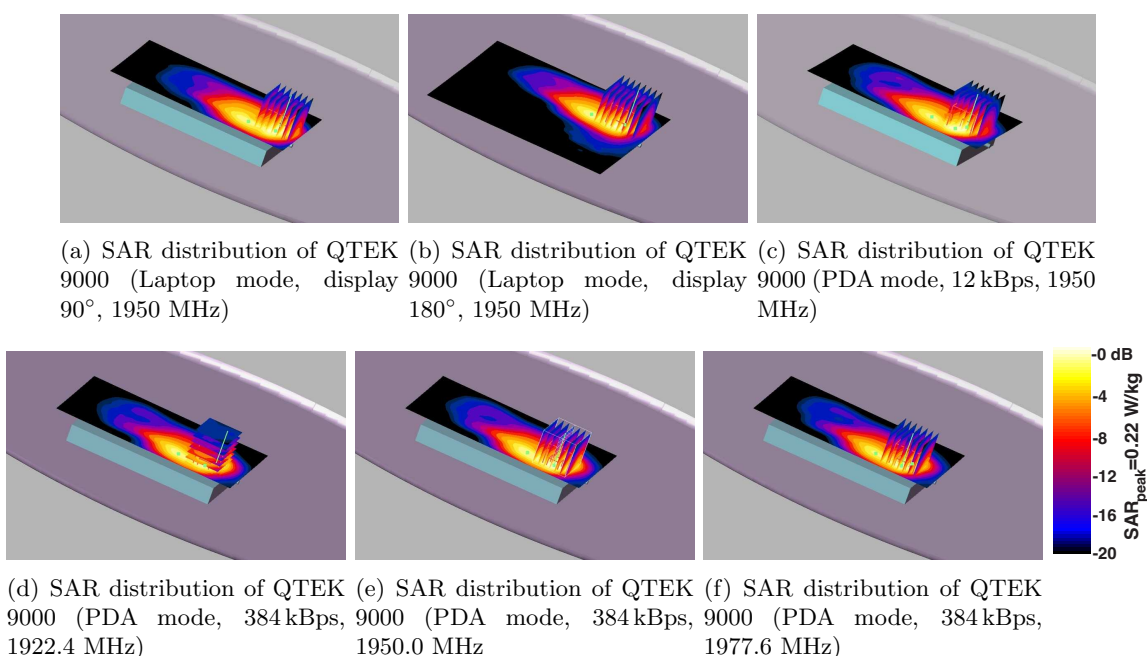
Figure 41: SAR distributions of the QTEK 9000 device in the UMTS band.

**EGPRS** The device was tested at maximum peak output power with two communication slot usage. The spatial average peak SAR results for the 900 MHz and 1800 MHz bands are summarized in Table 30. The corresponding SAR distributions are displayed in Figures 42, 43. The device has been tested in "laptop" and "PDA" modes attached to the phantom, as well as without the touch pad pen in PDA mode.

| DUT | f | SAR (W/kg) 1g | 10g | Configuration |
|---|---|---|---|---|
| **QTEK 9000** | **890.2** | **3.02** | **1.58** | **PDA, 2slot usage** |
| QTEK 9000 | 902.4 | 1.73 | 0.90 | PDA, 2slot usage |
| QTEK 9000 | 915.8 | 1.15 | 0.60 | PDA, 2slot usage |
| QTEK 9000 | 890.2 | 2.70 | 1.41 | PDA, without pen, 2slot usage |
| QTEK 9000 | 890.2 | 2.36 | 1.28 | Laptop 90, 2slot usage |
| QTEK 9000 | 890.2 | 2.28 | 1.26 | Laptop 180, 2slot usage |
| | | | | |
| **QTEK 9000** | **1710.2** | **3.41** | **1.45** | PDA, 2slot usage |
| QTEK 9000 | 1747.4 | 2.44 | 1.05 | PDA, 2slot usage |
| QTEK 9000 | 1784.8 | 1.16 | 0.71 | PDA, 2slot usage |
| QTEK 9000 | 1710.2 | 3.40 | 1.45 | PDA, without pen, 2slot usage |
| QTEK 9000 | 1710.2 | 2.71 | 1.24 | Laptop 90, 2slot usage |
| QTEK 9000 | 1710.2 | 2.71 | 1.23 | Laptop 180, 2slot usage |

Table 30: QTEK 9000 peak spatial average SAR in the EGPRS 900 and 1800 bands (maxima are bold).
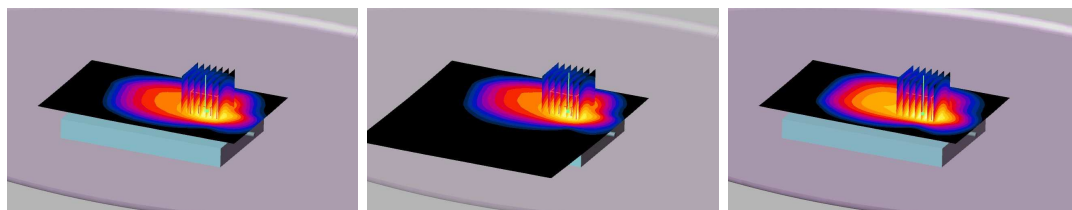


(a) SAR distribution of QTEK 9000 (Laptop mode, display 90°, 890.2 MHz)

(b) SAR distribution of QTEK 9000 (Laptop mode, display 180°, 890.2 MHz)

(c) SAR distribution of QTEK 9000 (PDA mode, touch pad pen removed, 890.2 MHz)
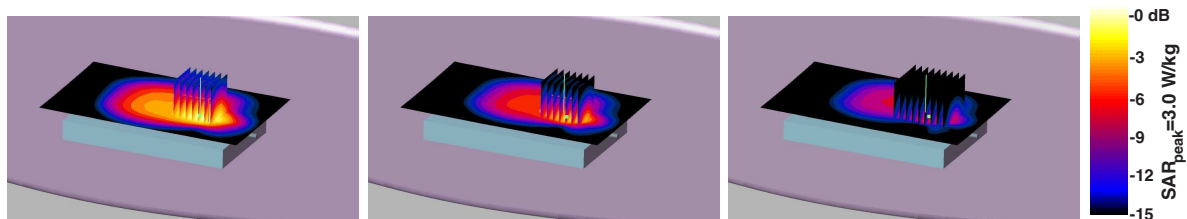
(d) SAR distribution of QTEK 9000 (PDA mode, 890.2 MHz)

(e) SAR distribution of QTEK 9000 (PDA mode, 902.4 MHz)

(f) SAR distribution of QTEK 9000 (PDA mode, 915.8 MHz)

Figure 42: SAR distributions of the QTEK 9000 device using the EGPRS 900 communication system (with 2 slot usage).
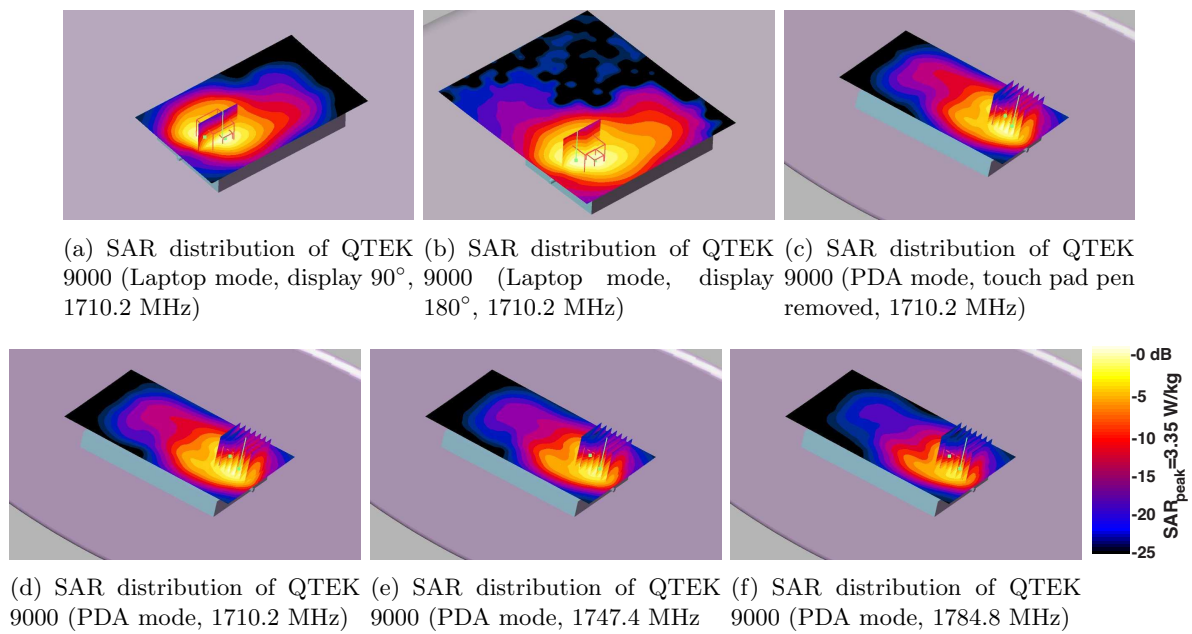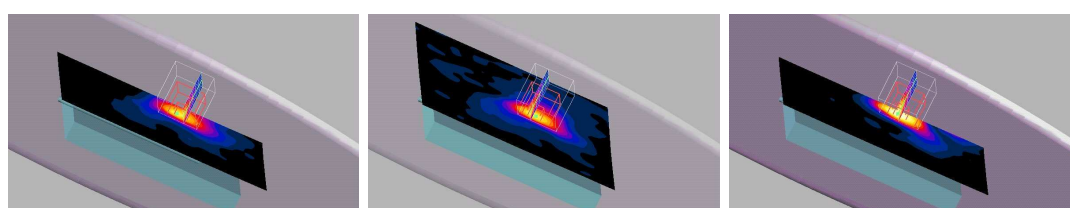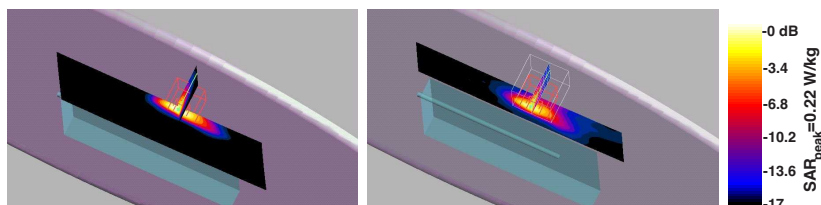
(a) SAR distribution of QTEK 9000 (Laptop mode, display 90°, 1710.2 MHz)

(b) SAR distribution of QTEK 9000 (Laptop mode, display 180°, 1710.2 MHz)

(c) SAR distribution of QTEK 9000 (PDA mode, touch pad pen removed, 1710.2 MHz)

(d) SAR distribution of QTEK 9000 (PDA mode, 1710.2 MHz)
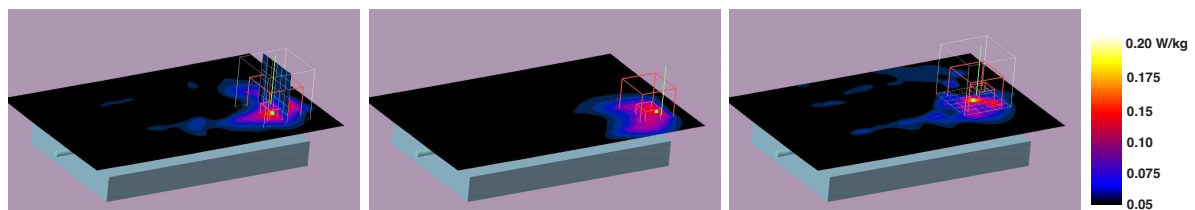
(e) SAR distribution of QTEK 9000 (PDA mode, 1747.4 MHz

(f) SAR distribution of QTEK 9000 (PDA mode, 1784.8 MHz)

Figure 43: SAR distributions of the QTEK 9000 device using the EGPRS 1800 communication system (with 2 slot usage).

**IEEE802.11b** The results of the dosimetric evaluation with a IEEE802.11b connection at maximum output power level are summarized in Table 31. Figure 44 displays the SAR distribution inside the tissue simulating liquids for the tested scenarios.

| | | SAR (W/kg) | | |
|---|---|---|---|---|
| **DUT** | **f** | **1g** | **10g** | **Configuration** |
| QTEK 9000 | 2412.0 | 0.163 | 0.070 | IEEE802.11b, data rate during test: 3.8Mbps, PDA |
| **QTEK 9000** | **2442.0** | **0.174** | **0.066** | IEEE802.11b, data rate during test: 3.8Mbps, PDA |
| QTEK 9000 | 2472.0 | 0.133 | 0.055 | IEEE802.11b, data rate during test: 3.8Mbps, PDA |
| QTEK 9000 | 2442.0 | 0.095 | 0.043 | IEEE802.11b, data rate during test: 3.8Mbps, Laptop, display 90 |
| QTEK 9000 | 2442.0 | 0.114 | 0.048 | IEEE802.11b, data rate during test: 3.8Mbps, Laptop, display 180 |

Table 31: QTEK 9000 peak spatial average SAR using the IEEE802.11b communication link (maximum is bold).



(a) SAR distribution of QTEK 9000 (Laptop mode, display 90°, 2442 MHz)

(b) SAR distribution of QTEK 9000 (Laptop mode, display 180°, 2442 MHz)

(c) SAR distribution of QTEK 9000 (PDA mode, 2412 MHz)



(d) SAR distribution of QTEK 9000 (PDA mode, 2442 MHz

(e) SAR distribution of QTEK 9000 (PDA mode, 2472 MHz)

Figure 44: SAR distributions of the QTEK 9000 device using the IEEE802.11b communication system.

**IEEE802.15.1** The results of the dosimetric evaluation with a IEEE802.15.1 connection at maximum output power level are summarized in Table 32. Figure 45 displays the SAR distribution inside the tissue simulating liquids for the tested scenarios.

| DUT | f | SAR (W/kg) | | Configuration |
|---|---|---|---|---|
| | | **1g** | **10g** | |
| **QTEK 9000** | **2440.0** | **0.016** | **0.0102** | IEEE802.11b, PDA |
| QTEK 9000 | 2440.0 | 0.012 | 0.009 | IEEE802.11b, Laptop, display 90 |
| QTEK 9000 | 2440.0 | 0.014 | 0.009 | IEEE802.11b, Laptop, display 180 |

Table 32: QTEK 9000 peak spatial average SAR using the IEEE802.15.1 communication link (maximum is bold).



(a) SAR distribution of QTEK 9000 (Laptop mode, display 90°, 2440 MHz)

(b) SAR distribution of QTEK 9000 (Laptop mode, display 180°, 2440 MHz)

(c) SAR distribution of QTEK 9000 (PDA mode, 2442 MHz)

Figure 45: SAR distributions of the QTEK 9000 device using the IEEE802.15.1 communication system.

### 8.4.2 Incident E&H-Fields

The incident E-field has been assessed for the Enterasys Roamabout RBT-4102 access point. The maximum E-field at a constant distance with the DUT rotating along three mutually perpendicular rotation axes has been previously determined; the E-fields were then mapped over distance in the maximum direction.

**E-GPRS** The measurements were taken in the 900 and 1800 MHz EGPRS bands. In order to preserve battery power over the measurement time, the measurements were taken at 29 and 26 dBm peak output power and extrapolated to the field strengths at 33 dBm and 30 dBm. The resulting E-field distributions are shown in Figures 46, 47. In the near field of the device the incident H-fields were determined as well. The results are displayed in Figures 48, 49.
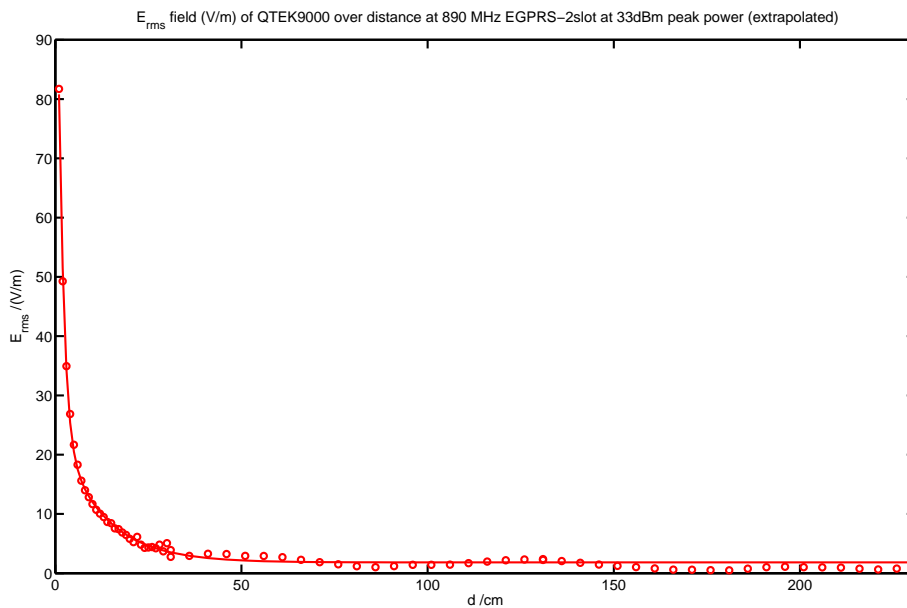


Figure 46: PDA E-field over distance (EGPRS900).
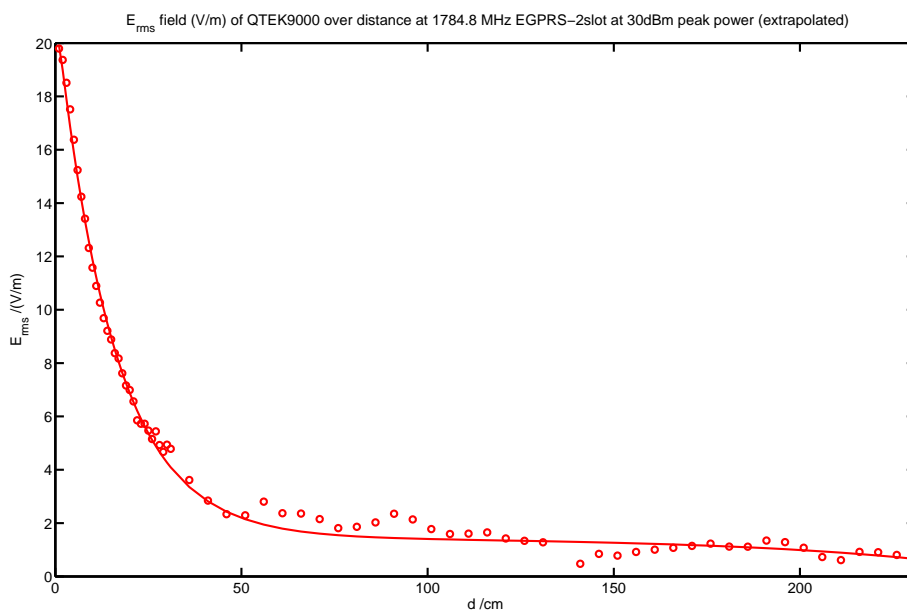


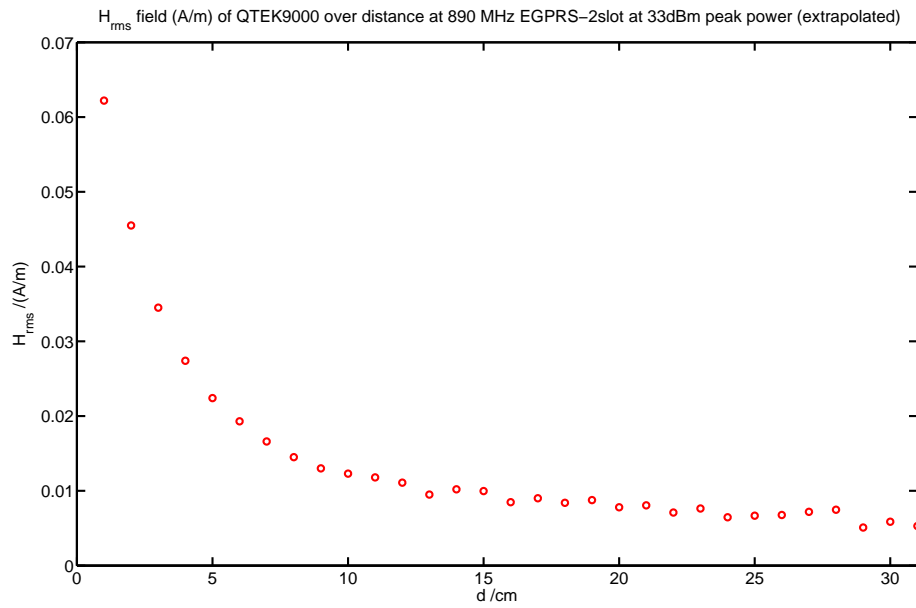Figure 47: PDA E-field over distance (EGPRS1800).
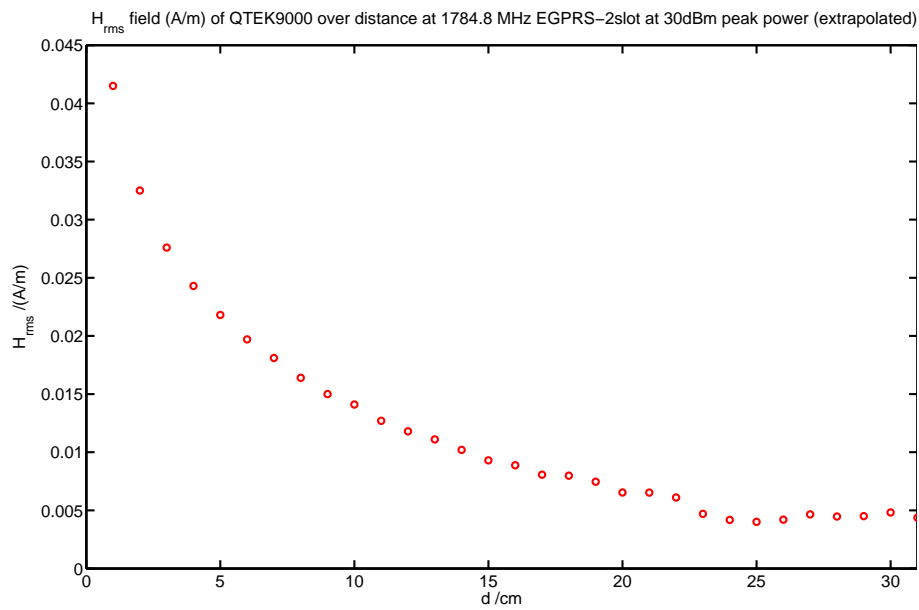
Figure 48: PDA H-Field over distance (EGPRS900).



Figure 49: PDA H-Field over distance (EGPRS1800).

**UMTS** The measurements were taken at maximum output power using the UMTS communication link. The resulting E-field distributions are shown in Figure 50. In the near field of the device the incident H-fields were determined as well. The results are displayed in Figure 51.
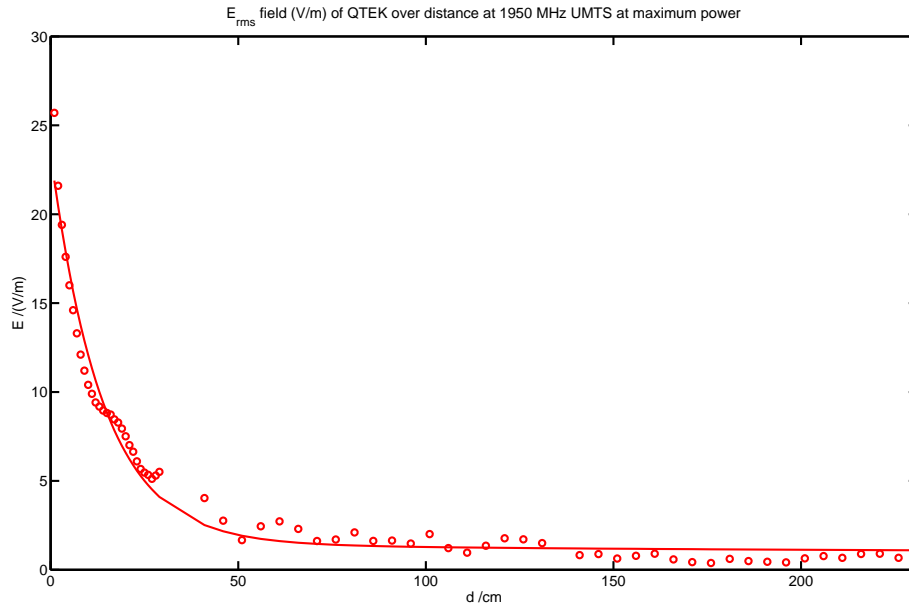


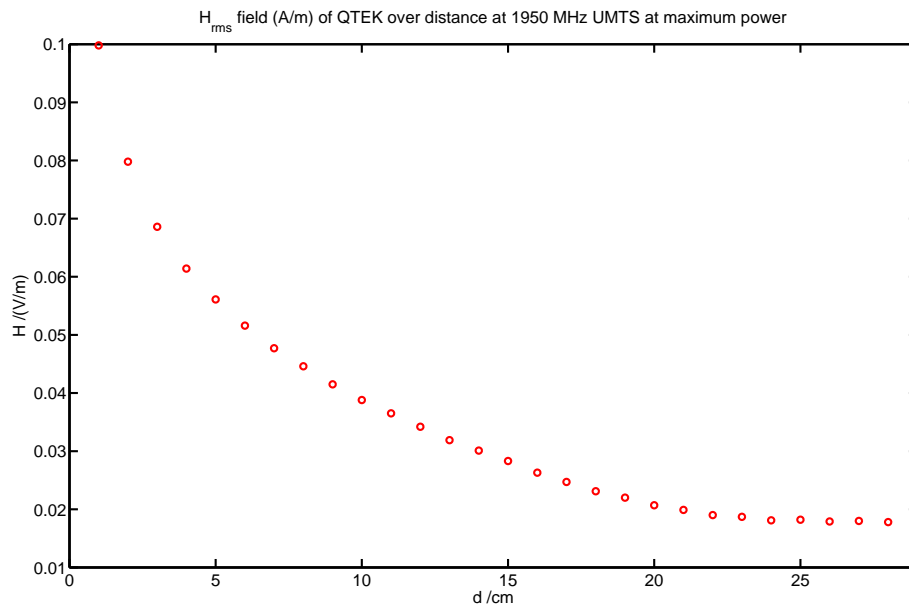Figure 50: PDA E-field over distance (UMTS).



Figure 51: PDA point H-Field over distance (UMTS).

**IEEE802.11b**  The measurements were taken at maximum output power in IEEE802.11b mode. The resulting E-field distributions are shown in Figure 52. In the near field of the device the incident H-fields were determined as well. The results are displayed in Figure 53.
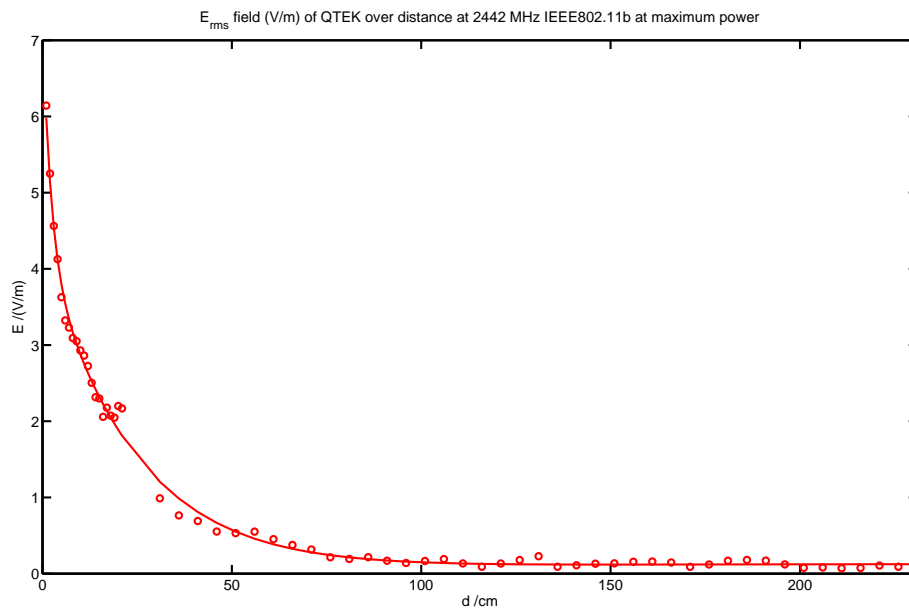


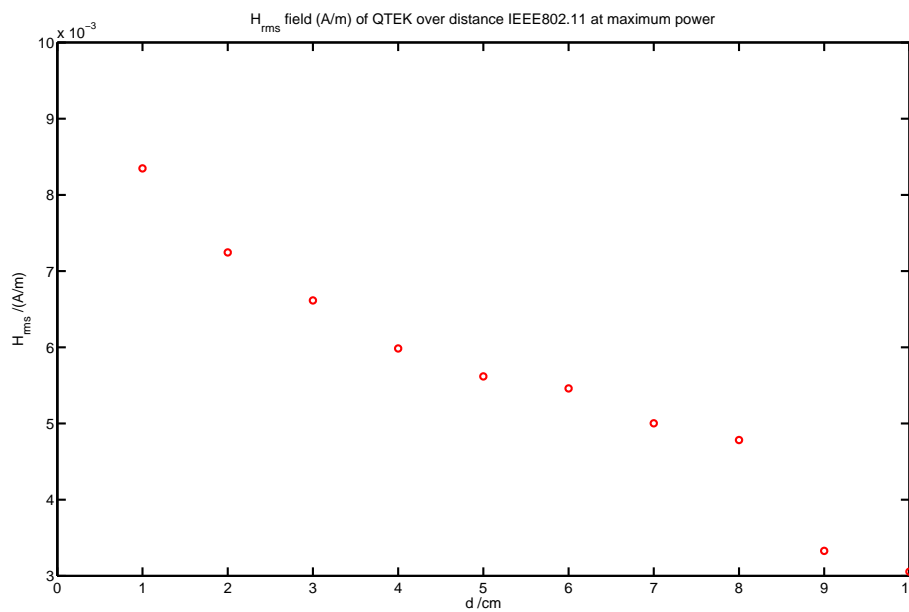Figure 52: PDA E-field over distance (IEEE802.11b).



Figure 53: PDA point H-Field over distance (IEEE802.11b).

**IEEE802.15.1** The measurements were taken at maximum output power in IEEE802.15.1 mode. The resulting E-field distribution is shown in Figure 54. The E-field could be mapped up to a distance of 130 cm only, since at further distances the PDA signal was dominated by the peer station signal. An attenuation of the peer signal was not possible without losing the connection. In the near field of the device the incident H-fields were determined as well. The results are displayed in Figure 55.
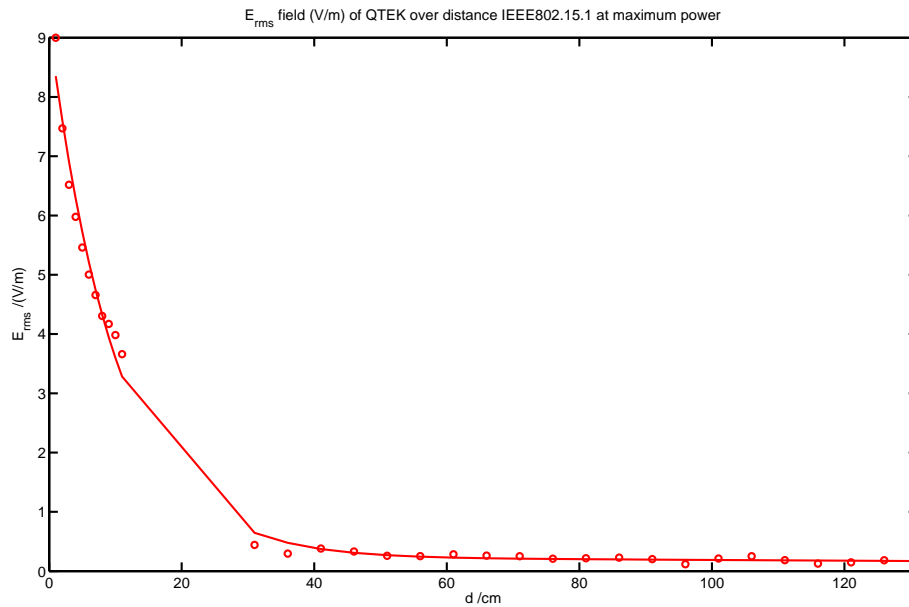


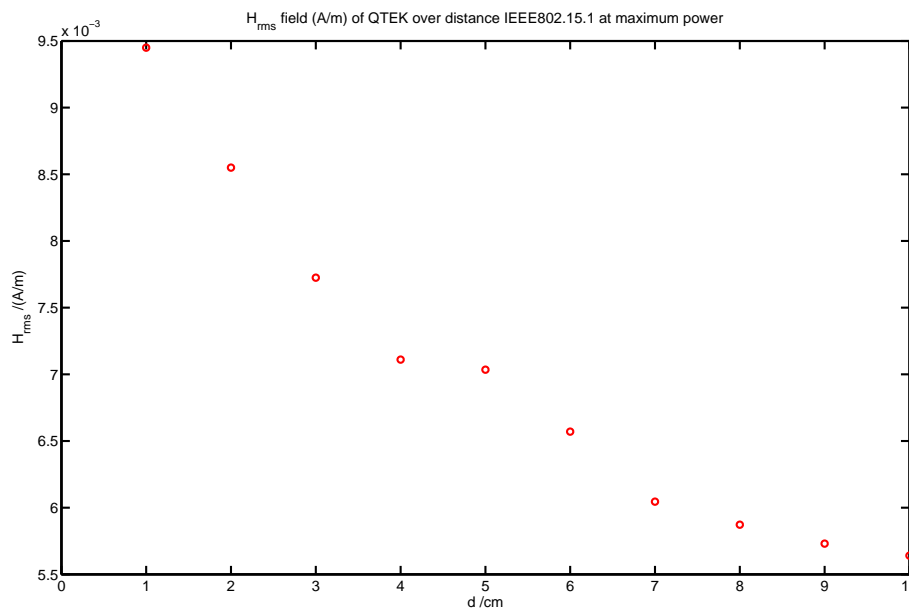Figure 54: PDA E-field over distance (IEEE802.15.1).



Figure 55: PDA point H-field over distance (IEEE802.15.1).

# 9   Discussion & Conclusions

The results from the peak spatial SAR assessments are summarized in Table 34. The results from the incident E-field assessment are summarized in Table 33. The presented results do not include the measurement and DUT uncertainty. Variation of the source – e.g., source output power stability, are included in the results. Specifically, some of the WLAN devices showed insufficient source stability if used in continuous transmission mode. Therefore the worst-case source variations (power drift) were added to the results. When testing WLAN devices, it is crucial to test the device in worst-case transmission mode, i.e., with maximum transmitted unidirectional data. We optimized the data throughput by determining the connection parameters for each DUT individually. Nevertheless, some uncertainty remains due to congestion in the communication channel and non-ideal behavior of the DUT baseband communication processors, as well as drivers and operating system delays.

The tested EGPRS devices support the multi-slot class 10, i.e., they were tested with two up-link slots occupied. Devices supporting more up-link slots are rarely available. Nevertheless, a maximum of four up-link slots occupied by a single device is possible for devices supporting the multi-slot class 12.

In conclusion, all of the tested devices were compliant with European peak spatial SAR limits, i.e., 2 W/kg for the head and trunk and 4 W/kg for limbs averaged over 10 g. The PDA showed peak spatial SAR values above the 2 W/kg limit. However, the tested orientation corresponds to usage in the hand; therefore the 4 W/kg limit has to be applied.

The close margin of the exposure of these devices with respect to the safety limits emphases that compliance can only be ensured if dosimetric compliance is demonstrated, e.g., following the procedures defined in this report. The maximum exposures within a radius of one two meters of the transmitters corresponds to typical exposures inside apartments close to base stations increasing the complexities of base station epidemiology.

| | $E_{rms}$ **(V/m)** | | | | | | | |
| | **5cm** | | **10 cm** | | **50 cm** | | **200 cm** | |
| **Communication System** | $E_{min}$ | $E_{max}$ | $E_{min}$ | $E_{max}$ | $E_{min}$ | $E_{max}$ | $E_{min}$ | $E_{max}$ |
|---|---|---|---|---|---|---|---|---|
| IEEE802.15.1 | 5.5 | | 4.0 | | 0.3 | | | |
| IEEE802.11b | 3.6 | 16.4 | 2.9 | 10.2 | 0.5 | 2.1 | 0.1 | 0.9 |
| IEEE802.11g | 1.9 | 5.0 | 1.3 | 3.1 | 0.4 | 0.6 | 0.2 | 0.3 |
| IEEE802.11a | 3.3 | 6.0 | 2.9 | 7.2 | 0.5 | 1.9 | 0.1 | 0.4 |
| EGPRS900 | 14.0 | 21.7 | 9.1 | 11.7 | 2.9 | 4.0 | 1.0 | 1.1 |
| EGPRS1800 | 10.0 | 16.4 | 7.8 | 11.6 | 1.3 | 2.3 | 0.7 | 1.1 |
| UMTS | 16.0 | 16.0 | 10.1 | 10.4 | 1.7 | 2.3 | 0.4 | 0.6 |

Table 33: Summary of the incident E-fields from wireless communication devices (Uncertainty (k=2): d≤20 cm $E_{rms}$ ±14.6% and for d>20 cm $E_{rms}$ ±31.2%).

| | peak spatial SAR (W/kg) | | | | | | | | | | | | | |
|---|---|---|---|---|---|---|---|---|---|---|---|---|---|---|
| | IEEE 802.11b | | IEEE 802.11g | | IEEE 802.11a | | UMTS | | EGPRS 900 | | EGPRS 1800 | | IEEE 802.15.1 | |
| | 1g | 10g | 1g | 10g | 1g | 10g | 1g | 10g | 1g | 10g | 1g | 10g | 1g | 10g |
| **Access Points** | | | | | | | | | | | | | | |
| Netgear ProSafe WG302 | 1.00 | 0.442 | 0.55 | 0.255 | | | | | | | | | | |
| ENTERASYS RBT-4102 | 1.47 | 0.73 | 0.58 | 0.274 | | | | | | | | | | |
| ENTERASYS RBT-4102 | | | | | 0.55 | 0.180 | | | | | | | | |
| Linksys WAG55 AG | | | | | 1.86 | 0.54 | | | | | | | | |
| Cisco Aironet 1200 RB | | | | | 0.419 | 0.100 | | | | | | | | |
| Cisco Aironet 1200 NRB | | | | | 1.59 | 0.359 | | | | | | | | |
| | | | | | | | | | | | | | | |
| **PDA** | | | | | | | | | | | | | | |
| QTEK 9000 | 0.174 | 0.67 | | | | | 4.17 | 2.06 | 3.02 | 1.58 | 3.40 | 1.45 | 0.016 | 0.010 |
| | | | | | | | | | | | | | | |
| **PC cards** | | | | | | | | | | | | | | |
| Netgear WAG511GE | | | | | 0.087 | 0.050 | | | | | | | | |
| Proxim ORiNOCO | | | | | 0.106 | 0.069 | | | | | | | | |
| 3Com XJACK | | | | | 0.072 | 0.063 | | | | | | | | |
| | | | | | | | | | | | | | | |
| Belkin F5D8010 | 0.77 | 0.425 | 0.185 | 0.105 | | | | | | | | | | |
| Globetrotter Fusion | 0.220 | 0.127 | 0.110 | 0.064 | | | | | | | | | | |
| | | | | | | | | | | | | | | |
| Globetrotter Fusion | | | | | | | 0.196 | 0.123 | 0.95 | 0.67 | 0.434 | 0.284 | | |

Table 34: Summary of the peak spatial SAR results from wireless communication devices (Uncertainty (k=2): $SAR_{1g}$ ±21% / $SAR_{10g}$ ±20.5% and for IEEE802.11a(5-6 GHz) $SAR_{1g}$ ±25.9% / $SAR_{10g}$ ±25.5%).

# References

[1] Axel Kramer, Sven Kühn, Urs Lott, and Niels Kuster. *Final Report:* Development of Procedures for the Assessment of Human Exposure to EMF from Wireless Devices in Home and Office Environments. Technical report, ETH-Zurich / IT'IS Foundation, Zeughausstrasse 43, 8004 Zurich, February 2005.

[2] IEC TC106. *Evaluation of Human Exposure to Radio Frequency Fields from Handheld and Body-Mounted Wireless Communication Devices in the Frequency Range of 30 MHz to 6 GHz (DRAFT)*, April 2004.

[3] IEEE Computer Society LAN MAN Standards Committee. *Part 11: Wireless LAN Medium Access Control (MAC) and Physical Layer (PHY) specifications*, August 1999.

[4] IEEE Computer Society LAN MAN Standards Committee. *Part 11: Wireless LAN Medium Access Control (MAC) and Physical Layer (PHY) specifications: Ammendment 4: Higher Data Rate Extension in the 2.4 GHz Band – Corrigendum 1*, November 2001.

[5] IEEE Computer Society LAN MAN Standards Committee. *Part 11: Wireless LAN Medium Access Control (MAC) and Physical Layer (PHY) specifications: Ammendment 4: Further Higher Data Rate Extension in the 2.4 GHz Band*, June 2003.

[6] IEEE Computer Society LAN MAN Standards Committee. *IEEE Trial–Use Recommended Practice for Multi-Vendor Access Point Interoperability via an Inter-Access Point Protocol Across Distribution Systems Supporting IEEE 802.11 Operation*, July 2003.

[7] IEEE Computer Society LAN MAN Standards Committee. *Part 11: Wireless LAN Medium Access Control (MAC) and Physical Layer (PHY) specifications: Higher–Speed Physical Layer Extension in the 5 GHz Band*, September 1999.

[8] IEEE Computer Society LAN MAN Standards Committee. *Part 11: Wireless LAN Medium Access Control (MAC) and Physical Layer (PHY) specifications: Ammendment 5: Spectrum and Transmit Power Management Extension in the 5 GHz band in Europe*, October 2003.

[9] OFCOM, Federal Office of Communications. Frequency characteristics and radio parameters (rlan). available WWW (07/02/2006): http://www.ofcomnet.ch/cgi-bin/rir.pl?id=1010, January 2006.

[10] J. Jun, P. Peddabachagari, and M. Sichitiu. Theoretical maximum throughput of IEEE 802.11 and its applications. In *Proc. 2nd IEEE Int'l. Symp. Net. Comp. and Applications*, pages 249–256, Cambridge, MA/UK, Apr. 2003.

[11] Ver. 1.2. *Specification of the Bluetooth System*, November 2003.

[12] Andreas Christ, Nicolas Chavannes, Neviana Nikoloski, Hans-Ulrich Gerber, Katja Poković, and Niels Kuster. A numerical and experimental comparison of human head phantoms for compliance testing of mobile telephone equipment. *Bioelectromagnetics*, 26(2):125–137, February 2005.

[13] SPEAG. "DASY4 Manual V4.5". Schmid & Partner Engineering AG, January 2006.